This document is confidential and is proprietary to the American Chemical Society and its authors. Do not copy or disclose without written permission. If you have received this item in error, notify the sender and delete all copies.

Unveiling the Role of Electrostatic Forces on Attraction between Opposing Polyelectrolyte Brushes

Journal:	Langmuir
Manuscript ID	la-2023-02762a.R2
Manuscript Type:	Article
Date Submitted by the Author:	n/a
Complete List of Authors:	Prusty, Debadutta; University of California Riverside, Department of Chemical and Environmental Engineering Gallegos, Alejandro; University of California Riverside, Department of Chemical and Environmental Engineering Wu, Jianzhong; University of California Riverside, Department of Chemical and Environmental Engineering

SCHOLARONE™ Manuscripts

Unveiling the Role of Electrostatic Forces on Attraction between Opposing Polyelectrolyte Brushes

Debadutta Prusty,[†] Alejandro Gallegos,[‡] and Jianzhong Wu*,[†]

†Department of Chemical and Environmental Engineering, University of California, Riverside, California 92507, USA

‡Division of Chemistry and Chemical Engineering, California Institute of Technology
Pasadena, Pasadena, California 91125, USA

E-mail: jwu@engr.ucr.edu

Abstract

Electrostatic interaction and molecular excluded-volume effects are responsible for a plethora of non-intuitive phenomena in soft-matter systems including local charge inversion and attraction between similar charges. In the current work, we study the surface forces and swelling behavior of opposing polyelectrolyte brushes using a classical density functional theory that accounts for electrostatic and excluded-volume correlations. We observe that the detachment pressure between similarly charged brushes is sensitive to salt concentration in both the osmotic and salted regimes and can be negative in the presence of multivalent counterions. A comparison of the theoretical results with the mean-field predictions unravels the role of correlation effects in determining the surface forces and the brush structure. For systems containing multivalent counterions, the detachment pressure attains negative values at an intermediate brush-brush separation, and the attractive region in the pressure-vs-distance plot is magnified in

terms of both the depth and width of attraction with increasing the counterion valency. However, the inter-brush attraction vanishes when the size-induced correlations are switched off. We also investigate the role of counterion size and the polymer chain length on the detachment pressure. It is found that smaller counterions are more effective in neutralizing the polymer charge than bigger counterions, leading to a reduced inter-brush repulsion and in some cases, attraction between like-charged brushes at intermediate distances. Meanwhile, varying the chain length of the grafted polymers only shifts the location of the attraction basin with little influence on the interaction strength. The theoretical predictions show a qualitative agreement with experimental observations and offer valuable insights into interaction between similarly charged polymer brushes in the presence of multivalent ions.

Keywords—Brush-brush interaction, Multivalent counterions, Classical density functional theory, Electrostatic correlation, Monomer-counterion crosslinks, Excluded-volume interactions

Introduction

Correlation effects due to electrostatic interactions and the excluded volume of ionic species are typically ignored in mean-field calculations but are responsible for a myriad of non-trivial phenomena in soft-matter systems. ^{1,2} Such effects become particularly prominent for systems containing multivalent ions as well as for monovalent electrolytes at high ion concentrations. ^{3–5} The presence of multivalent ions may induce charge inversion near electrified walls, ^{6,7} adsorption of polyelectrolytes onto a like-charged surface, ^{8–10} reversible swelling and collapse of polymer gels, ¹¹ and the condensation of a high molecular weight DNA into a compact state. ^{12,13}

In polyelectrolyte brush systems, the addition of multivalent counterions results in the strong shrinkage of the polymer brush compared to that with only monovalent counterions.¹⁴ Because multivalent counterions exhibit stronger electrostatic attraction with oppo-

sitely charged polyelectrolytes, they can neutralize the polymer charge more effectively than monovalent counterions, leading to both inter- and intra-chain bridging and heterogeneous collapse of polyelectrolyte brushes at low grafting densities. ¹⁵ Furthermore, multivalent ions may induce attraction between like charged nanoparticles 16-19 and planar walls. 20 Multivalent ions are also responsible for the dramatic increase of friction between opposing polyelectrolyte brushes sliding against each other. 21 The interaction between similarly charged polymer brushes is relevant to technological applications such as boundary lubrication in medical devices and colloidal stabilization. ^{22,23}

When opposing polymer brushes of the same charge are brought together in a good solvent, the inter-brush interaction is governed by multiple factors. ²³ First, at small distances, there are effects associated with the increase of counterion concentration and excluded volume interactions due to physical contacts between both the same and opposing brush monomers, which generate strong steric repulsion between the brushes.²⁴ Second, the brushes will be compressed due to the electrostatic repulsion between like-charged monomers belonging to the opposing brushes, which localizes the monomers near their respective grafting surfaces. ²⁵ Furthermore, the localization of polymer segments due to tethering limits intermixing between apposing chains. Lastly, there is a balance of elastic effects associated with the polymer conformation and the inter-chain repulsion among monomers of the same brush that dictates the swelling of the opposing polymer brushes. Depending on the inter-brush distance, either of these aforementioned factors can be dominant in determining the inter-brush interaction.

Interestingly, due to the presence of an extra brush compared to a single brush system, a competition between multiple salt-mediated phenomena sets in. In addition to screening the electrostatic repulsion and reducing osmotic pressure, multivalent counterions can become intercalated between the oppositely charged monomers due to enhanced electrostatic attraction. ^{21,24} This 'bridging' phenomenon can lead to two effects. First, it can collapse the brushes individually, moving them away from each other. 24,26 Second, it can interlink two opposing brushes that are overlapping.²⁴ The competition between these two effects would be influenced by the counterion valence, size and polymer chain length.²⁴ The experimental investigations by Yu et al. revealed different electrostatic effects on the structural properties of polyelectrolyte brushes for counterions of the same valency but different sizes.²⁷ In addition, chain length was found to be an important factor in determining the interdigitation and normal force between brushes in monovalent salt systems.²⁸ Furthermore, it was demonstrated that, in the presence of multivalent counterions, variations in grafting density in single-wall brush systems can either extend or contract the polymer chains.²⁹ Considering the strong inter-connection between chain extension and electrostatic and excluded-volume repulsion, we anticipate that, in opposing brush systems, grafting density will play a crucial role in influencing the interaction between the opposing brushes.

A substantial theoretical literature exists on the interaction between opposing polyelectrolyte brushes. Numerical results from molecular dynamics (MD) simulation showed different scaling regimes in terms of the disjoining pressure versus the separation between brushes. 30,31 A significant depression of the monomer concentration was observed in the weakly interpenetrated regime, and the monomer concentration becomes virtually uniform for a large degree of interpenetration. 32 A transition of the brush structure was discovered from polymer-in-good-solvent behavior at low grafting densities to melt-like behavior at high grafting densities. 30 The simulation results also indicated that the disjoining pressure was mainly influenced by the osmotic pressure of counterions at large distances, and by steric interactions at small separations, 30 as well as by the distortion of the polyelectrolyte chains in response to the ionic environment.³³ The dependence of the interpenetration length on the polymer chain length and brush-brush distance identified by simulation was found in good agreement with scaling analysis.³² Dissipative particle dynamics (DPD) was also used to examine the dependence of the brush height on the charge fraction and the lubricantion properties of polyelectrolyte brushes.³⁴ Zhulina and Borisov²⁵ derived an analytical strong-stretching theory (SST) and predicted that, in the presence of monovalent ions, the interaction between opposing brushes is always repulsive and that the compression of semi-

dilute brushes in a salt-free theta solvent leads to the reduction of the brush thickness and a polymer-free region to mitigate the electrostatic repulsion. Later Matsen³⁵ carried out a comparative study of the SST predictions with a self-consistent field theory (SCFT) that accounts for fluctuation effects. He observed that SST predicts brush contraction to maintain a polymer-free gap, while SCFT reveals that fluctuations, ignored in the former approach, extend the chains out, leading to a higher degree of interpenetration between the polymer brushes. In a subsequent publication, ²⁸ the same author incorporated salt effects into the analysis and found that a lower salt concentration enhances both the repulsion between brushes and interpenetration. Zhulina and Rubinstein³⁶ investigated the sliding behavior of a salt-free opposing polyelectrolyte brush system using scaling arguments. It was observed that for intermediate and high grafting densities, both the shear stress and the normal stress are larger in the brush system than in a system of bare walls with the same charge density. However, the increase in normal forces between opposing polyelectrolyte brushes, as compared to the forces between bare charged surfaces, is notably more significant, leading to a reduced friction coefficient. A reverse behavior was observed in the low grafting density regime. Wang and Tong³⁷ used a two-dimensional self-consistent field theory to study opposing strong polyelectrolyte brushes of varying fractions of charged segments. At large brush-brush separations, these authors observed a positive correlation of the brush height, and hence the polymer interpenetration, with the polymer charge fraction, grafting density and chain length. At small brush-brush separations, both quantities became insensitive to the above parameters due to the brush shrinkage to reduce the inter-brush repulsion, corroborating the findings from earlier works as discussed before.

The aforementioned theoretical investigations were mostly focused on monovalent counterions, and naturally they predict that the interaction between opposing polyelectrolyte brushes is always repulsive. To our knowledge, theoretical exploration of multivalent ion effects on interaction between polyelectrolyte brushes has been limited. MD simulations by Cao and coworkers²⁶ investigated inter-brush interactions mediated by both trivalent and monovalent counterions. In the presence of trivalent counterions, the brushes experienced significant contraction at larger distances, attributed mainly to ion condensation onto the charged chains. Conversely, at shorter distances, the simulation results show a reduction in pressure. As for continuum approaches, the lack of investigation on multivalent systems may be attributed to the fact that most theoretical frameworks including SCFT rely on the Poisson-Boltzmann equation to calculate the electrostatic potential. The mean-field approach fails to represent the ionic excluded-volume effects and electrostatic correlations that are known to be important for systems containing multivalent ions. A recent work by Nap and Szleifer²⁴ tried to accommodate monomer-counterion correlations within the framework of the molecular theory. The mean-field approach accounts for the correlation effects by modelling counterion condensation as chemical reaction. Specifically, two types of chemical reactions are assigned to capture the ability of calcium ions to form complexes with one and two negatively charged monomers. With the corresponding reaction constants calibrated with results from MD simulations or experimental reports, it was shown that the addition of a small amount of calcium ions was able to change the inter-brush interaction from being repulsive to attractive at certain inter-brush separations.

The theoretical investigation of opposing brushes under multivalent ion conditions is far from conclusive. The aforementioned approach by Nap and Szleifer²⁴ considered weak polyelectrolytes and involved acid dissociation equilibrium competing with counterion condensation. A strong polyelectrolyte system in this regard would better facilitate isolating the role of counterion-monomer correlations. Also, it might not be feasible to obtain condensation equilibria data for all specific counterions. However, hydration radius data is available in the literature for most counterions and therefore, a theory accounting for size-induced correlations directly would allow linking the collapse behavior to counterion and chain structural attributes, making clear the general physics prevailing in these systems. To this end, classical density functional theory (cDFT) provides an effective approach since it captures both excluded volume and electrostatic correlations explicitly.³⁸ Previously, cDFT has proved use-

ful for describing electrostatic phenomena in a variety of soft matter and ionic systems such as surface forces due to confined polyelectrolyte chains, ³⁹ oscillatory charge distributions in ionic liquids, ⁴⁰ and the swelling behavior of single-wall polyelectrolyte brushes. ^{29,41} It is with this prior success of the technique in mind that we, in the current work, use cDFT to study the structural and interfacial properties of opposing polyelectrolyte brushes in different salt systems.

The remainder of this paper is organized as follows. In the section "Molecular Model and Theory", we describe our model system and the key cDFT equations used in this work. The next section discusses the theoretical predictions. Specifically, first, we present the effect of salt concentration on the detachment pressure for monovalent, divalent and trivalent ions and compare the theoretical results with mean-field predictions to gauge the importance of correlation effects. We also analyze the density profiles of counterions and monomers, interdigitation amount and electrostatic potential profiles to understand the structural origin of the observed inter-brush interactions. In a similar way, we discuss the effects of grafting density and polymer chain length. This is followed by a study on the variation of the size of counterions and its effects on the detachment pressure. While a direct comparison of our theoretical results with experimental data is difficult because the chain lengths used in experiments are significantly higher, aside from other differences in system parameters such as the grafting density and the architecture of polymer chains, we find good qualitative agreement between the theoretical results and experimental observations with regard to the general trends such as the effect of salt concentration and valency on the brush thickness and inter-brush potential.

Molecular Model and Theory

The molecular model for polyelectrolyte brushes is similar to that used in our previous studies. ^{29,42} The system comprises two opposing polyelectrolyte brushes parallel to each other

immersed in an aqueous electrolyte solution containing monomeric ionic species. We assume that the segment densities and other distance-dependent quantities in the system, such as the electrostatic potential and ionic distributions, vary only in the direction perpendicular to the substrates, taken to be the z direction. This assumption of lateral homogeneity is usually justified when the average distance between neighboring grafting locations is less than the radius of gyration of the polymer chains in their unattached state.

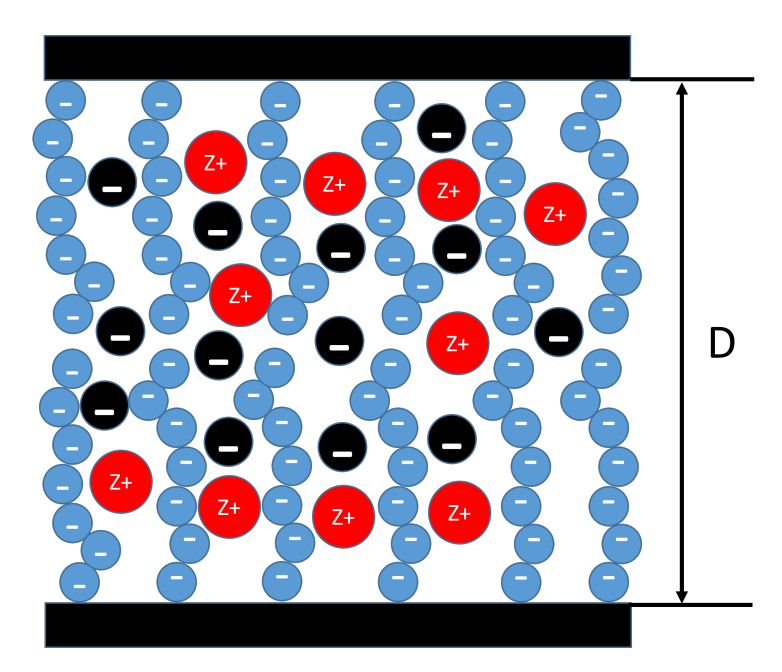


Figure 1: Schematic of the opposing polyelectrolyte brushes. Here, D denotes the separation between two grafting substrates, and Z_+ represents the counterion valence. The polymer segments and coions are assumed monovalent.

Schematically, Figure 1 presents the tethered polymers and salt ions confined between two parallel plates representing the grafting surfaces. The solvent is described as a continuum background with a relative dielectric constant of $\epsilon_r = 78$, which corresponds to that for liquid water at room temperature. The surface-to-surface distance between the two plates is designated as D, and the grafting density of the polymer chains is defined as $\sigma_g = n_P/A$, where A is the surface area of each plate, and n_P is the number of grafted chains per plate. The entire system is in contact with a reservoir of a salt solution at bulk concentration c_S . The salt is made of spherical ions, denoted by MX_Z , where $Z = Z_+$ is the valency of

counterions, i.e., salt ions with an electrostatic charge different from that of the tethered chains. The coion, X, is treated as monovalent $Z_{-} = -1$.

For simplicity, all monomeric species are represented by charged hard spheres with the same diameter, $\sigma_P = 0.425$ nm. In other words, the polymer segments (P), cations (M) and anions (X) have the same size unless stated otherwise. Each polymer chain consists of N_P negatively charged monovalent monomers with one end attached to a uncharged solid substrate. The monomers and salt ions interact with each other through a combination of the Coulomb energy and a hard-core potential as described in the primitive model of electrolyte solutions:

$$\beta u_{ij}(\mathbf{r}_{ij}) = \begin{cases} \infty, & r_{ij} < \sigma_P, \\ l_B Z_i Z_j / r_{ij}, & r_{ij} \ge \sigma_P \end{cases}$$
 (1)

where $l_B = \beta e^2/(4\pi\epsilon_0\epsilon_r) \approx 0.714$ nm is the Bjerrum length, Z_i and Z_j are ion valences, $r_{ij} =$ $|\mathbf{r}_{ij}|$ is the center-to-center distance between ionic species i and j, and ϵ_0 is the permittivity of the free space. As usual, $\beta = 1/(k_B T)$, where T is the temperature in kelvin and k_B is the Boltzmann constant.

The cDFT for representing the thermodynamic properties of the brush system has been reported in our earlier work. ²⁹ The essential task in cDFT calculation is to solve the density profiles of all ionic species and the electric potential by minimizing the grand potential:

$$\Omega = F - \int d\mathbf{r} \rho_M(\mathbf{r}) [\mu_M - V_M^{ext}(\mathbf{r})] - \int d\mathbf{r} \rho_X(\mathbf{r}) [\mu_X - V_X^{ext}(\mathbf{r})]$$

$$+ \int d\mathbf{R} \rho_{P_1}(\mathbf{R}) V_{P_1}^{ext}(\mathbf{R}) + \int d\mathbf{R} \rho_{P_2}(\mathbf{R}) V_{P_2}^{ext}(\mathbf{R})$$
(2)

where $\mathbf{R} = (\mathbf{r}_1, \mathbf{r}_2, \mathbf{r}_3, ..., \mathbf{r}_{N_P})$ is defined by the positions of all monomers of a single chain hence representing a particular polymer configuration, μ_M and μ_X are the chemical potentials of the cation and the anion, respectively, P_1 and P_2 denote the polymer chains from the opposing brushes, $V_i^{ext}(\mathbf{r})$ is the external potential capturing the hard core interactions of species i with the two grafting plates. For each monomeric species, the external potential is given by

$$\beta V_i^{ext}(\mathbf{r}) = \begin{cases} \infty, & z < \sigma_P/2 \text{ or } z > D - \sigma_P/2 \\ 0, & \text{otherwise.} \end{cases}$$
 (3)

In Eqn.(2), F denotes the intrinsic Helmholtz energy, which can be written as a summation of the ideal and excess contributions³⁸

$$F = F_{id} + F_{ex}. (4)$$

The ideal part of the intrinsic Helmholtz energy accounts for the conformational entropy of polyelectrolyte chains in the brush and the translational degrees of freedom for the salt ions. Formally, this term is exactly known:

$$\beta F_{id} = \int d\mathbf{R} \rho_{P1}(\mathbf{R}) \Big\{ \ln[\rho_{P1}(\mathbf{R})] - 1 \Big\} + \int d\mathbf{R} \rho_{P2}(\mathbf{R}) \Big\{ \ln[\rho_{P2}(\mathbf{R})] - 1 \Big\}$$

$$+ \int d\mathbf{R} \rho_{P1}(\mathbf{R}) \beta V_{P1}^b(\mathbf{R}) + \int d\mathbf{R} \rho_{P2}(\mathbf{R}) \beta V_{P2}^b(\mathbf{R})$$

$$+ \int d\mathbf{r} \rho_M(\mathbf{r}) \Big\{ \ln[\rho_M(\mathbf{r})] - 1 \Big\} + \int d\mathbf{r} \rho_X(\mathbf{r}) \Big\{ \ln[\rho_X(\mathbf{r})] - 1 \Big\}$$

$$(5)$$

The first two terms on the right side of Eqn.(5) account for the conformational entropic free energies of polymer chains grafted to surface 1 and surface 2, the third and fourth terms are related to the bonding potentials of the polymer chains, and the fifth and sixth terms arise from the translational entropies of the cations and anions, respectively. The logarithm terms in this equation reflect the Boltzmann distribution for different conformations of non-interacting polymer chains. Because the conformational probability is a multi-dimensional function depending on the position of individual polymer segments, there is no simple connection between the logarithm terms and the elasticity of a single polymer chain.

According to our model, the excess part of the intrinsic Helmholtz energy, F_{ex} , includes contributions from excluded volume interactions among all monomeric species, the electrostatic interactions, and correlations effects due to electrostatic-hard-sphere coupling and

chain connectivity. 43 The expressions for these contributions are well-established and reproduced in the Supporting Information (SI) for completeness.

Minimizing the grand potential given by Eqn.(2) yields the expressions for solving the density profiles of monomeric species and the electrostatic potential. The equation for the polymer conformational density, $\rho_P(\mathbf{R})$, of a particular polymer brush $P = P_1$ or P_2 , reads as:

$$\ln \rho_P(\mathbf{R}) = \ln K - \beta V_P^b(\mathbf{R}) - \beta \sum_{i=1}^{N_P} \lambda_i(\mathbf{r}_i) - \beta V_P^{ext}(\mathbf{R})$$
 (6)

where $\lambda_i(\mathbf{r}) = \delta F_{ex}/\delta \rho_i(\mathbf{r})$ stands for the one-body potential for segment i of the polymer chain, and the constant K is determined by normalization conditions applied to all polymer segments, i.e., $\int_0^D dz \rho_{iP}(z) = \sigma_g$ with $\rho_{iP}(z)$ being the local density of polymer segment i from brush P. The local monomer density follows from the polymer conformational density by integration over the positions of polymer segments:

$$\rho_{P}(\mathbf{r}) = \sum_{i=1}^{N_{P}} \rho_{iP}(\mathbf{r}) = \sum_{i=1}^{N_{P}} \int d\mathbf{R} \delta(\mathbf{r} - \mathbf{r}_{i}) \rho_{P}(\mathbf{R})$$

$$= K \left\{ \delta(z - z_{g}) + \sum_{i=2}^{N_{P}} \exp\left[-\beta \lambda_{i}(\mathbf{r})\right] G_{iP}^{L}(\mathbf{r}) G_{iP}^{R}(\mathbf{r}) \right\}$$
(7)

where $G_{iP}^L(\mathbf{r})$ and $G_{iP}^R(\mathbf{r})$ are the propagator functions for the polymer chains from brush P, and $\delta(z)$ represents the Dirac delta function. In the second line of Eqn.(7), the first term accounts for attaching an end segment to the surface; its density is proportional to a delta function since this monomer is fixed at the corresponding grafting surface $(z_g = \sigma_P/2 \text{ for } P_1 \text{ and } z_g = D - \sigma_P/2 \text{ for } P_2)$.

With the assumption of lateral homogeneity, the density profile varies only in the z direction and hence, the propagator expressions can be simplified as

$$G_{iP}^{L}(z) = \int dz' \exp[-\beta \lambda_i(z')] \frac{\Theta(\sigma_P - |z - z'|)}{2\sigma_P} G_{(i-1)P}^{L}(z)$$
(8)

$$G_{iP}^{R}(z) = \int dz' \exp[-\beta \lambda_i(z')] \frac{\Theta(\sigma_P - |z - z'|)}{2\sigma_P} G_{(i+1)P}^{R}(z)$$
(9)

where $G_{N_PP}^R(z) = 1$, $G_{2P}^L(z) = \exp[-\lambda_2(z_g)]\Theta(\sigma_P - |z - z_g|)/(2\sigma_P)$, and $\Theta(z)$ stands for the Heaviside function. The boundary condition relating to the second monomer, $G_{2P}^L(z)$, reflects the fact that the first monomer is fixed at the surface of the corresponding plate and hence, experiences a one-body potential equal to infinity everywhere except the grafting location. The total monomer density, $\rho_p(z)$, consists of contributions from the monomer densities of both brushes, i.e., $\rho_p(z) = \rho_{P_1}(z) + \rho_{P_2}(z)$. The density profiles for mobile species (viz., coions and counterions) are calculated from the modified Boltzmann equation

$$\rho_{\alpha}(z) = \frac{1}{\Lambda_{\alpha}^{3}} \exp\{-\beta [V_{\alpha}^{ext}(z) + \lambda_{\alpha}(z) - \mu_{\alpha}]\}$$
(10)

where Λ_{α} is the thermal wavelength, $\lambda_{\alpha}(\mathbf{r}) = \delta F_{ex}/\delta \rho_{\alpha}(\mathbf{r})$, and μ_{α} is the chemical potential of species α in the bulk.

We used the Picard iteration to solve for the density profiles.²⁹ The stopping criterion was that, at each value of z, the difference in the local densities between two successive iterations was less than 10^{-6} times the corresponding bulk densities for mobile species and the difference in surface densities was less than 10^{-6} times the corresponding grafting densities for the polymer chains. Because the ideal part of the free energy corresponding to the polymer requires scanning over the positions of all monomers, the computation of the grand potential from Eqn.(2) is not straightforward and hence, we seek a simplification of the expression. Plugging in the expression for the conformation density in Eqn.(6) into Eqn.(2) yields the ideal intrinsic Helmholtz energy due to the tethered polymer chains:

$$\beta F_{id}^{P} = 2n_{P}(\ln K - 1) - \beta \int d\mathbf{r} [\rho_{P_{1}}(\mathbf{r})\lambda_{P_{1}}(\mathbf{r})] - \beta \int d\mathbf{r} [\rho_{P_{2}}(\mathbf{r})\lambda_{P_{2}}(\mathbf{r})]$$

$$= 2n_{P}(\ln K - 1) - 2\beta \int d\mathbf{r} \rho_{p}(\mathbf{r})\lambda_{p}(\mathbf{r})$$
(11)

The last line in the above equation follows the same identity of monomers of chains P_1 and P_2 . Here, n_P is the number of polymer chains as defined earlier and, in one-dimensional computation, it gets normalized to the grafting density (σ_g) . Similarly, substituting the expression for the density profiles of free ions $(\alpha = M, X)$ into Eqn.(2) gives

$$\beta F_{id}^{\alpha} = -\int dz \rho_{\alpha}(z) \beta \lambda_{\alpha}(z) - \int dz \rho_{\alpha}(z)$$
 (12)

These two expressions enable us to write the grand potential as

$$\beta\Omega = \beta F_{id}^P + \beta F_{id}^\alpha + \beta F_{ex} \tag{13}$$

Again, the explicit expression for βF_{ex} is presented in the Supporting Information.

We see from the above discussion that cDFT explicitly accounts for the excluded volumes of all ionic species and their correlations with electrostatic interactions and intra-chain connectivity, thereby allowing us to explore effects arising from sizes and valencies of ionic species. As was mentioned in the introduction, ionic correlations may lead to non-monotonic swelling in the single-brush polyelectrolyte system among other non-intuitive phenomena. ²⁹ To study its role in the interaction between opposing brushes, we will analyze the changes in thermodynamic and structural properties as the separation between brushes is varied under different salt conditions.

Results and Discussion

The primary quantity of interest in this study is the detachment pressure, defined as the external pressure applied on two grafting plates in order to keep them at a particular interplate distance. A positive value of the detachment pressure signifies repulsion between the opposing brushes, and a negative value means inter-brush attraction.

Mathematically, the detachment pressure corresponds to the negative of the derivative

of the grand potential per unit area with respect to distance minus the pressure of the corresponding the non-interacting plates:⁴⁴

$$\beta P(D) = -\frac{1}{A} \left\{ \frac{\partial \beta \Omega}{\partial D'} \Big|_{D'=D} - \frac{\partial \beta \Omega}{\partial D'} \Big|_{D'=\infty} \right\}$$
 (14)

In determining the detachment pressure from the above equation, it is not numerically possible to calculate the grand potential at an infinite inter-plate separation. When the separation between two opposing brushes is sufficiently large, the grand potential would vary linearly with the distance since the only change in it would be due to additional mobile species, whose free energy density is constant. This is so because at such distances, the opposing brushes stop interacting with each other and the density profiles have already achieved their bulk values in the midplane between the two plates.

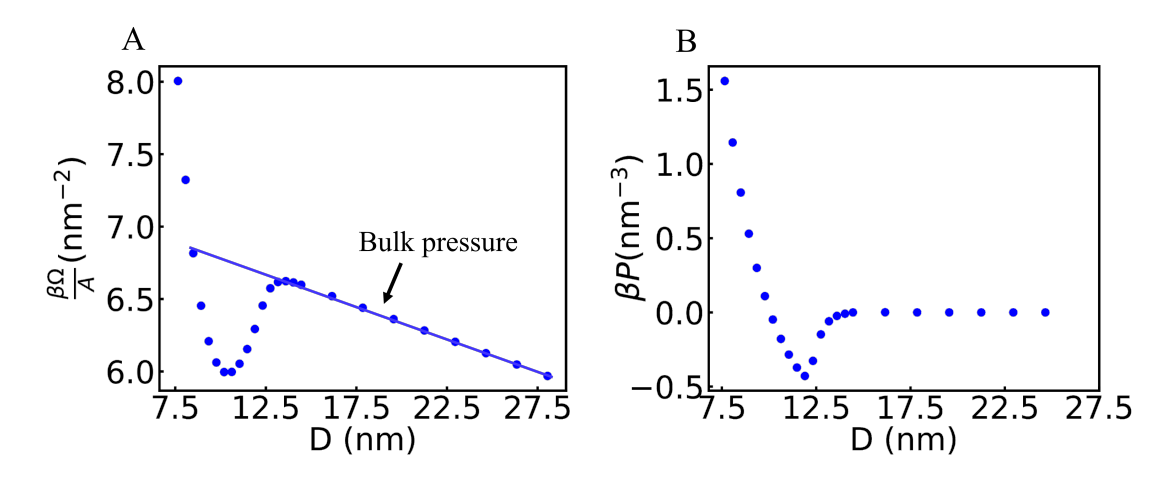


Figure 2: An illustrative example for calculating the detachment pressure between opposing brushes. (A) The variation of the grand potential with the inter-plate distance D. The slope at large values of D gives the bulk pressure. (B) The detachment pressure versus D generated from the numerical differentiation of the grand potential. Here, the salt contains trivalent counterions at a concentration of 25 mM, the polymer chain length is $N_P = 30$, and the grafting density is 0.4 nm^{-2} .

As an illustrative example, Figure 2 shows the numerical procedure for calculating the detachment pressure using Eqn.(14). First, we calculate the grand potential for two opposing brushes at a set of inter-brush distances. Here, each polymer chain contains $N_P = 30$ charged

segments, the grafting density is $\sigma_g = 0.4 \text{ nm}^{-2}$, and the two brushes are surrounded by a salt solution with trivalent cations at salt concentration $c_S = 25 \text{ mM}$. Next, the corresponding pressure curve is constructed by numerical derivative as given in the right panel of Figure 2. It is clear that the slope is constant at high values of inter-plate distance D and hence the detachment pressure would be zero. As the inter-brush distance D is reduced, the interaction between the opposing brushes gives rise to a non-zero value of the reduced detachment pressure βP .

Effect of salt concentration

We first consider the effects of salt concentration on the detachment pressure between two polyelectrolyte brushes at a fixed polymer grafting density of $\sigma_g = 0.4 \text{ nm}^{-2}$ and chain length $N_P = 30$. Figure 3 shows the variation of the detachment pressure with the interplate distance at different concentrations of monovalent counterions. We also include in the same plot a comparison with mean-field predictions at low salt concentrations, which were achieved by turning off the short-range correlation terms (both excluded volume and electrostatic correlations).

Although the repulsion profiles for interactions between opposing brushes of the same charge are somewhat anticipated, the theoretical findings unveil a multitude of interesting features. Both classical DFT and mean-field analysis predict that the salt concentration has virtually no influence on the detachment pressure at low and intermediate salt concentrations (upto 250 mM). This is probably not obvious at first sight because salt ions are expected to have strong screening effects on interaction between similarly charged surfaces. According to the conventional theories of colloidal interactions, a significant reduction of the electrostatic interactions would be expected as the salt concentration increases. The non-intuitive behavior can be understood by recapitulating the conclusions from the seminal works on opposing polyelectrolyte brushes by Pincus²³ and Zhulina. These pioneering works predict the invariance of the separation pressure with respect to salt concentration when the

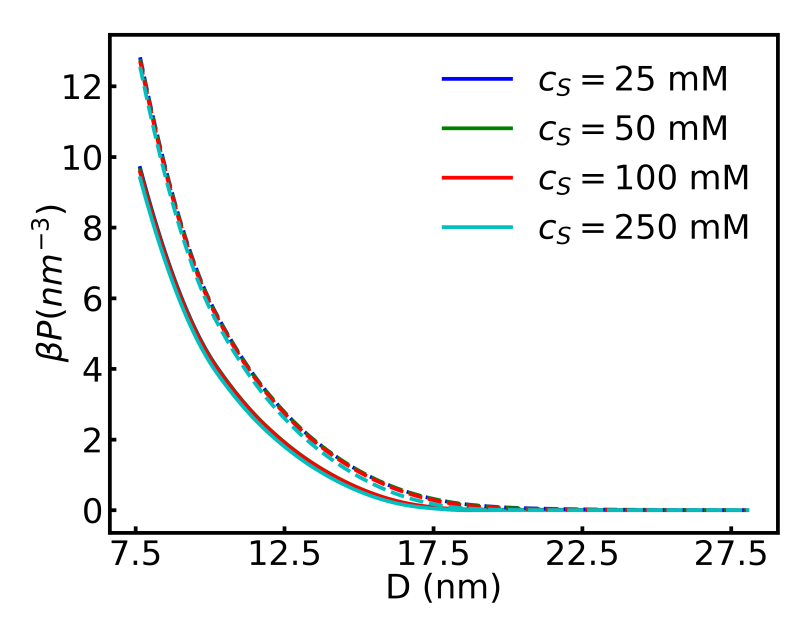


Figure 3: Variation of the detachment pressure with the inter-plate distance (D) for interaction between opposing brushes surrounded by monovalent counterions at different salt concentrations (C_S) . The solid lines represent cDFT predictions and the dashed lines are mean-field predictions. Here, the polymer chain length is $N_P = 30$, and the grafting density is $\sigma_q = 0.4 \text{ nm}^{-2}$.

average counterion concentration in the brush is significantly larger than that of salt ions in the bulk. This condition characterises what is known as the "osmotic brush" regime. Under such circumstances, the Debye screening length, which is inversely proportional to the ion concentration, corresponding to the confined counterion (κ^{-1}) is sufficiently smaller than the corresponding length associated with salt ions (κ_S^{-1}) .²³ For the grafting density of polymers considered in this work (0.4 nm^{-2}) , κ^{-1} evaluates to approximately 0.35 nm, while κ_S^{-1} varies between 0.85 nm and 4.35 nm. This suggests that the brushes considered in this work fall into the osmotic regime. As the polymer charge in the brush is completely neutralized by counterions, the counterion concentration in the brush is insensitive to the bulk salt concentration.

Another way to explain the insensitivity of the separation pressure towards the salt concentration would be to consider the average counterion concentration inside the brush. At large inter-plate distances, the average counterion concentration in the brush reaches the

lowest value since at smaller distances, more counterions penetrate into the inter-plate region and thus the counterion concentration increases due to the overlap between the opposing brushes. For the salt conditions shown in Figure 3, the counterion density inside the brush varies little with the bulk concentration. The average value computes to approximately 1 nm⁻³ in terms of the number density, which translates to 1670 mM. Note that only free ions in the brush, not the ones condensed on charged monomers, contribute to the osmotic pressure; hence the cross-over concentration would be lower than the above value. Nevertheless, 1670 mM is significantly higher than the salt concentrations for systems shown in Figure 3. As a result, the brush stays in the osmotic regime, displaying insensitivity of the detachment pressure to the salt concentration.

To provide evidence for the validity of the above argument, Figure S3 gives βP vs c_S curves, going up to a slightly higher concentration of the salt, 1000 mM. It is clear that in going from 250 mM to 1000 mM, both the range and the magnitude of the interaction decrease significantly, indicating a cross-over to the salted brush regime. Qualitatively, the theoretical predictions align well with the main conclusions of previous experimental observations. For example, Balastre et al. prepared several polyelectrolyte brushes by the adsorption of amphiphilic diblock copolymers consisting of poly(tert-butylstyrene) and sodium poly(styrenesulfonate) (PtBS-NaPSS) on a mica surface through the hydrophobic attraction of PtBS. 45 The surface force apparatus (SFA) measurements for the brush-brush interaction in NaNO₃ solutions indicated that, at low bulk salt concentrations, the disjoining pressure was insensitive to the ionic strength. The absence of electrostatic double-layer forces in the osmotic regime is fully consistent with our cDFT predictions as shown in Figure 3. At low salt conditions, the force profiles are close to each other due to the high monomer concentration in the osmotic brush regime. As previously reported, 42 cDFT predicts the decrease of the brush height upon the further increase of the ionic strength in the bulk, suggesting a reduced brush-brush repulsion at a fixed distance as shown in Figure S3.

Similar SFA measurements on opposing brushes made of diblock poly(tert-butyl methacrylate)-

b-poly(glycidyl methacrylate sodium sulfonate)(PtBMA-PGMAS) in NaCl solution showed a weak dependence of the brush-brush interaction on salt concentration at long distances. ⁴⁶ The force-distance curves merge into a single profile at small distances regardless of the salt concentration, indicating the dominance of steric repulsion. At higher distances, there was an inverse dependence on salt concentration distinctively different from electric double layer forces. Atomic force microscopy measurements on sodium poly(styrenesulfonate) (PSS) brushes in NaCl solution ^{47,48} and poly allylaminehydrochloride (PLL) in NaCl solution also exhibited the same trend with respect to salt concentration. ⁴⁹ As shown in Figure S4, plotting our data on a log-log scale reveals the sensitivity of the detachment pressure to the salt concentration at large distances, which cannot be seen in Figure 3 due to extremely small values of the pressure. Nevertheless, the long-range brush-brush interaction is clearly different from that for the electrostatic interaction between similarly charged surfaces.

Optical tweezer measurements on poly(2-vinylpyridine) (P2VP) grafted SiO_2 colloids in KCl solution revealed that, when the brush is fully charged at low pHs, the brush-brush interaction was insensitive to the salt concentration while at intermediate pHs, where the brush is partially charged, the interaction force is reduced upon the addition of the salt.⁵⁰ In the latter case, the responsiveness of the brush-brush interaction to salt addition is due to the fact that a reduced polymer charge at high pHs corresponds to a lower threshold concentration for the transition from osmotic brush regime to salted brush regime. Although a quantitative comparison is not possible with these results since the chain lengths used in the above studies is significantly higher (> 130) than the values used in the current work, the cDFT predictions capture the general trends in terms of salt concentration effects on the brush swelling and brush-brush interactions.

The invariance of the detachment pressure with the salt concentration in the "osmotic brush" regime is additionally corroborated by the counterion density profiles for different salt concentrations. As shown in Figure 4 for two opposing brushes at small and large separations, the counterion density profiles superimpose onto each other in the brush region. Under the

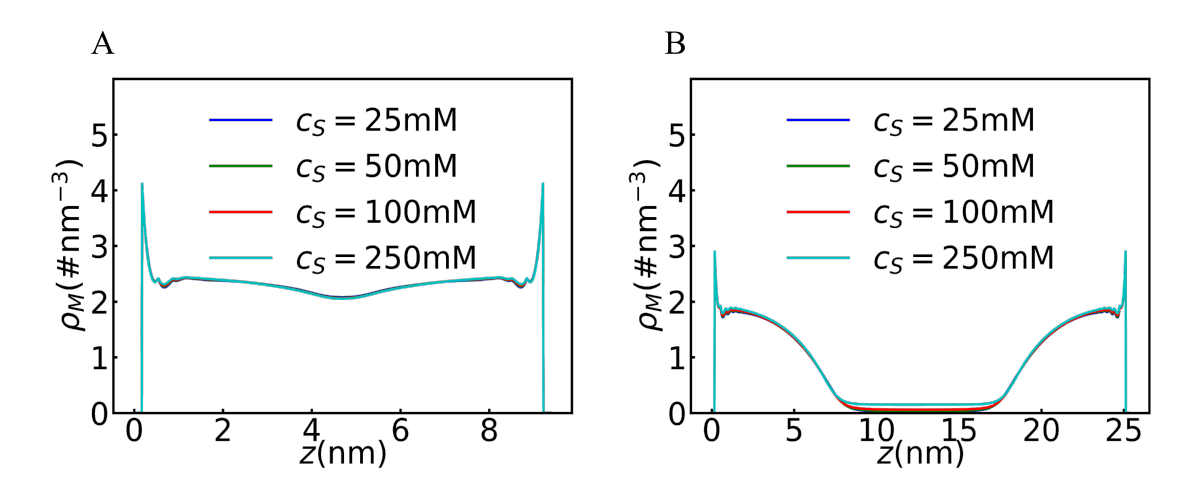


Figure 4: The counterion density profiles at different salt concentrations for inter-plate distance (A) D = 11 nm (B) D = 29.7 nm. As in Figure 3, the counterions are monovalent, the polymer chain length is $N_P = 30$, and the grafting density is $\sigma_g = 0.4$ nm⁻².

osmotic brush conditions, $^{30,36} \beta P$ is predicted to vary as D^{-2} at large separations, as D^{-1} at intermediate separations, and as D^{-3} at extremely small separations where excluded volume interactions become dominant. As is shown in Figure S3 of SI, an attempt at fitting the obtained curves to the powers of D yielded -3.3 at only small Ds for all salt concentrations and values between -4 and -5 at higher Ds depending on the salt concentration. When the short-range correlations were switched off, the power values obtained are significantly lower, due probably to the enhancement of long-range part of the inter-surface interactions. Nevertheless, the fact that all the obtained values are greater than 3 in magnitude indicates that the decay of pressure at large inter-brush distances is not long-range in nature, signifying the difference between opposing charged brush systems and opposing bare surface systems. A possible explanation for the observed deviation between cDFT and the previous scaling analysis could be the neglect of electrostatic correlations, both short range and long range in the work on brushes and the neglect of short-range correlations in bare charged surface systems. The first two powers of D, -2 at large separations and -1 at intermediate separations, were derived by assuming the ideal gas behavior for salt ions, and the third power, -3 at extremely small separations, by using only excluded volume interactions. Returning to the comparison between cDFT and mean-field predictions, although the results from the two theoretical methods are qualitatively similar, correlation effects are non-negligible even for monovalent systems at low salt concentration as reflected in the drastic reduction of the inter-brush repulsion. When short-range correlations are considered, the observed pressure is significantly reduced compared to the mean-field predictions.

Effect of counterion valence

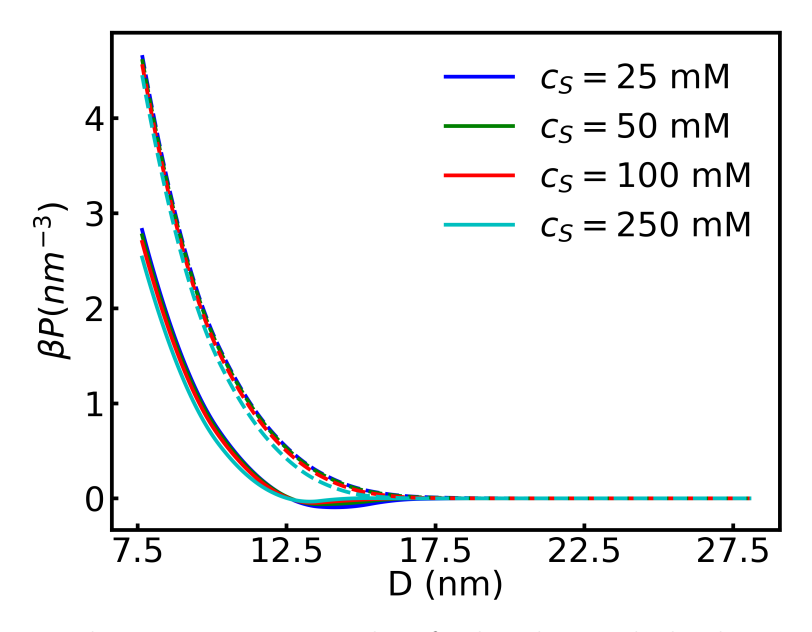


Figure 5: The same as Figure 3 but for brushes with divalent counterions.

For systems containing divalent and trivalent counterions, the difference between cDFT and mean-field predictions becomes even more pronounced. Figures 5 and 6 show the detachment pressure versus the distance in the presence of divalent and trivalent counterions, respectively. In both cases, the detachment pressure takes on negative values at intermediate distances, indicating attraction between similarly charged polyelectrolyte brushes. This attraction is most noticeable for the lowest salt concentration (25 mM) and the magnitude is enhanced by increasing the counterion valency. Regarding the dependence of detachment pressure on the concentration of multivalent counterions, it is possible to identify two distinct regimes of the brush-brush interaction. In the first regime, which occurs at short inter-plate

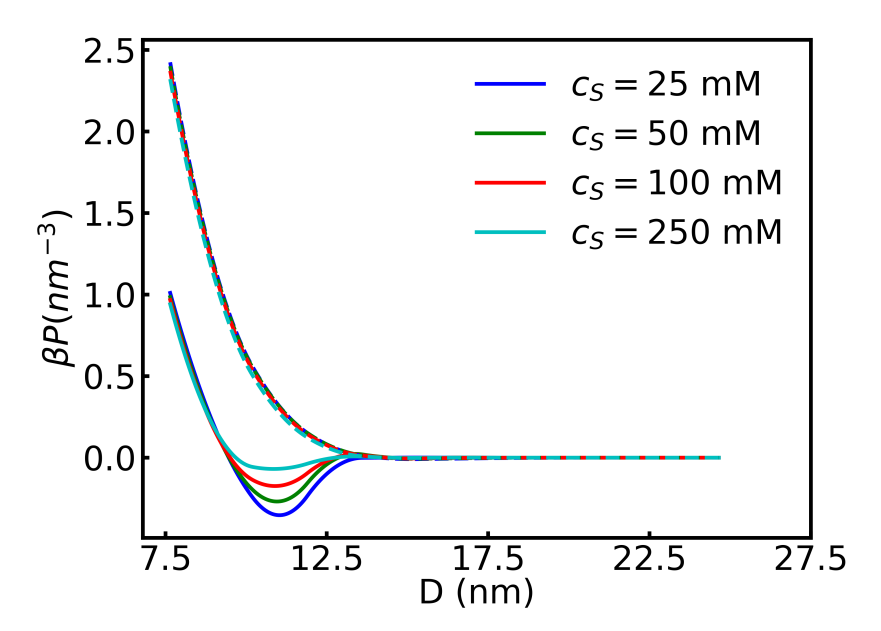


Figure 6: The same as Figure 3 but for brushes with trivalent counterions.

separation, the overlap between opposing brushes enhances the excluded volume effects and the magnitude of electrostatic repulsion. In this case, the detachment pressure is relatively insensitive to the concentration of multivalent counterions. Because the amount of counterions in the inter-plate region remains almost unchanged for different salt concentrations, the weak salt concentration effect indicates the dominance of the excluded volume repulsion of the polymer segments over electrostatic screening due to salt ions. This observation is intuitive and in qualitative agreement with experimental results. For example, addition of Y^{3+} to NaNO₃ was shown to reduce the pressure between opposing poly styrene sulphonate brushes.²⁷ The second regime occurs at intermediate distances, which is associated with attractive interactions in the presence of multivalent counterions. In the experiments reported by Yu et al.,²¹ the brush-brush attraction is manifested in an increase in friction coefficient and has been attributed to counterions linking to the monomers of opposing brushes. In this regime, we observe an inverse correlation between attractive pressure and salt concentration, as can be seen from the reduced depth of the attractive region at high salt concentrations and a slight increase in the distance of crossover from attraction to repulsion with increas-

ing salt concentration shown in Figure 6. At first glance, this trend seems surprising since a higher amount of counterions would be expected to facilitate more bridging. However, adding more counterions to the system also contracts the brushes individually, inhibiting intimate overlap between brushes and hence, reducing the number of inter-brush interlinks. This reduced number of interlinks results in shallower attractive valleys for brush-brush interactions at higher salt concentrations. As will be discussed later, this argument is supported by the monomer density profiles corresponding to the minimums in βP vs D curves under trivalent ion conditions. We speculate at this point that there is a crossover from an inter-brush-bridging-dominated regime to an intra-brush-bridging-dominated dominated regime with increasing salt concentration. To study this in more detail, we will discuss in a later section how the detachment pressure varies with the concentration of multivalent ions at a fixed concentration of a monovalent salt (NaCl).

Figures 7 and 8 compare the monomer and counterion density profiles predicted by cDFT and the mean-field approximation for monovalent and trivalent systems at D=9.4 nm and $c_S=25$ mM. Here, the salt concentration and the inter-brush separation correspond to the maximum attraction in the trivalent system. The reduction of the detachment pressure with the increase of the counterion valency can be attributed to a combination of two factors. First, a higher valency means a lesser number of counterions required to neutralize the brush. The electroneutrality effect is evident from a comparison of the density profiles for monovalent counterions, shown in Figure 7, with those for trivalent ions shown in Figure 8. This reduced counterion concentration is responsible for a decreased pressure due to excluded volume interactions. Second, the electrostatic correlation, which is primarily attractive, is higher for systems with counterions of higher valencies, which also reduces the detachment pressure.

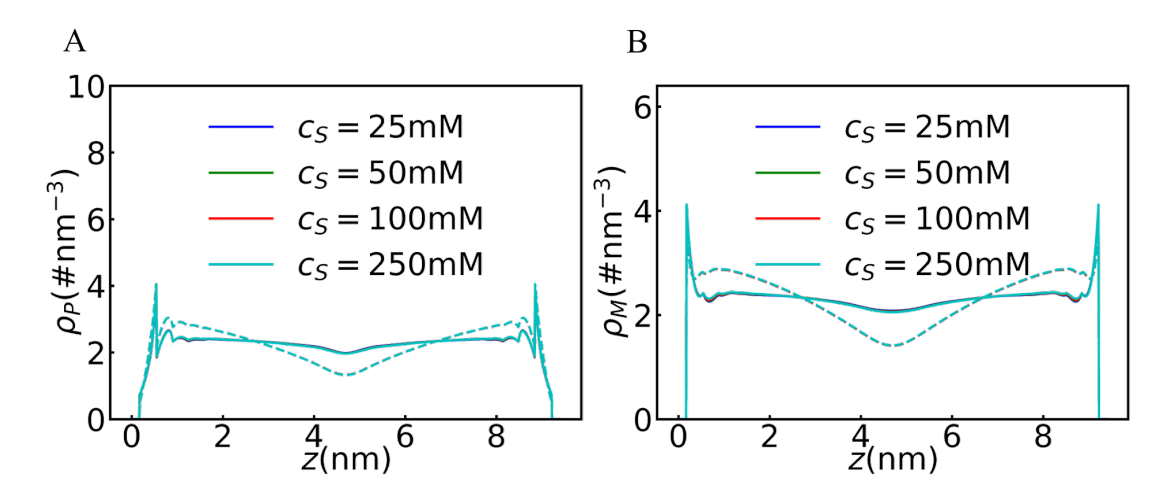


Figure 7: The density profiles of monomers (A) and monovalent counterions (B) between two opposing polyelectrolyte brushes. Here D=9.4 nm. The solid lines represent cDFT predictions and the dashed lines are mean-field predictions.

Brush height and interdigitation

To further understand the structural origin of attraction between opposing polyelectrolyte brushes, we have analyzed the variation of brush height with separation and the density profiles of monomers and counterions. The brush height can be calculated from the density profile of polymer segments:⁵¹

$$H = \frac{2\int_0^D dz z \rho_P(z)}{\int_0^D dz \rho_P(z)} \tag{15}$$

where $\rho_P(z)$ is the density of monomers from an individual brush, not the density of monomers from two brushes combined. To quantify the overlap between two brushes, we also compute the degree of interdigitation, which is defined as the cumulative monomer density of a brush extending beyond the mid-plane normalized by the total amount of monomer of a brush:²⁶

$$\Gamma_g = \frac{\int_{D/2}^{D} dz \; \rho_P(z)}{\int_{0}^{D} dz \; \rho_P(z)} \tag{16}$$

The left panels in Figures 9 and 10 give the brush height versus inter-plate distance for the same systems considered in the previous section. The results from both cDFT and the mean-field approach are presented for comparison. For both valencies, the brush heights

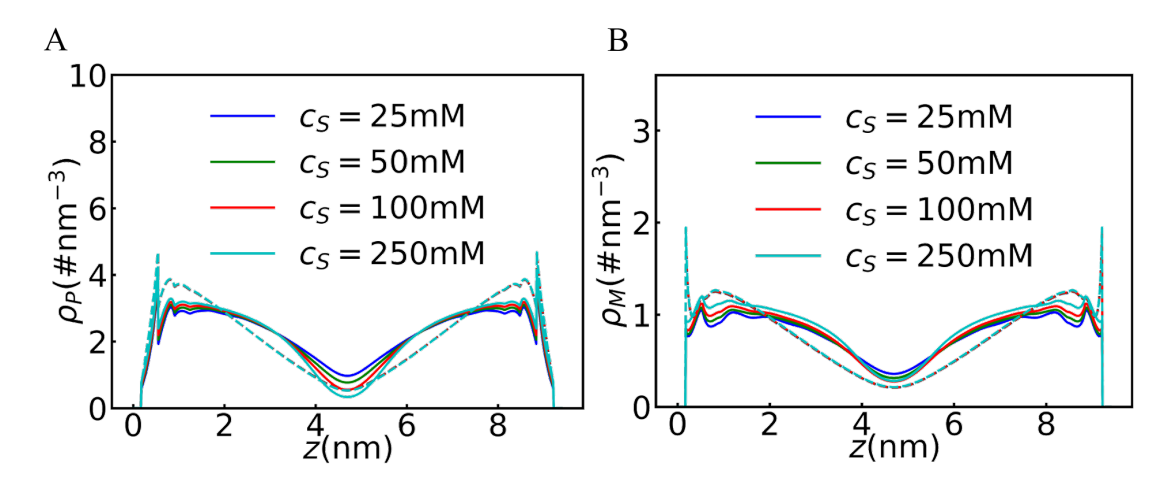


Figure 8: Monomer density profiles (A) and counterion density profiles (B) for a system with trivalent counterions at D = 9.4 nm. The solid lines represent cDFT predictions and the dashed lines are mean-field predictions.

predicted by cDFT are greater than the mean-field predictions. This is an excluded volume driven effect since electrostatic correlations collapse polyelectrolyte brushes²⁷ while excluded volume effects lead to polymer elongation, increasing the brush height. It is also seen from these figures that at large distances, the brush height is lower for trivalent counterions than that for monovalent counterions. The simple reason for this is that trivalent ions screen the electrostatic repulsion between charged monomers more effectively. Besides, they can also form bridges between charged monomers, causing the brush to collapse. As far as salt concentration effects are concerned, at large inter-plate distances, the brush height increases slightly with decreasing salt concentration. As the inter-brush separation is reduced, the effects of salt concentration become negligible and, for the reasons discussed before, the curves for all salt concentrations collapse into one profile.

Figure 10 shows that the salt concentration effects on the brush heights are more pronounced in the trivalent ion case, which exhibits a noticeable upward blip at intermediate distances. However, such effects are not captured by the mean-field theory, which instead shows a monotonic increase of the brush height with the inter-plate separation. Clearly, the non-monotonic behavior emerges only when correlations are taken into consideration. This re-entrant behavior of the brush expansion is closely related to the extension of the individ-

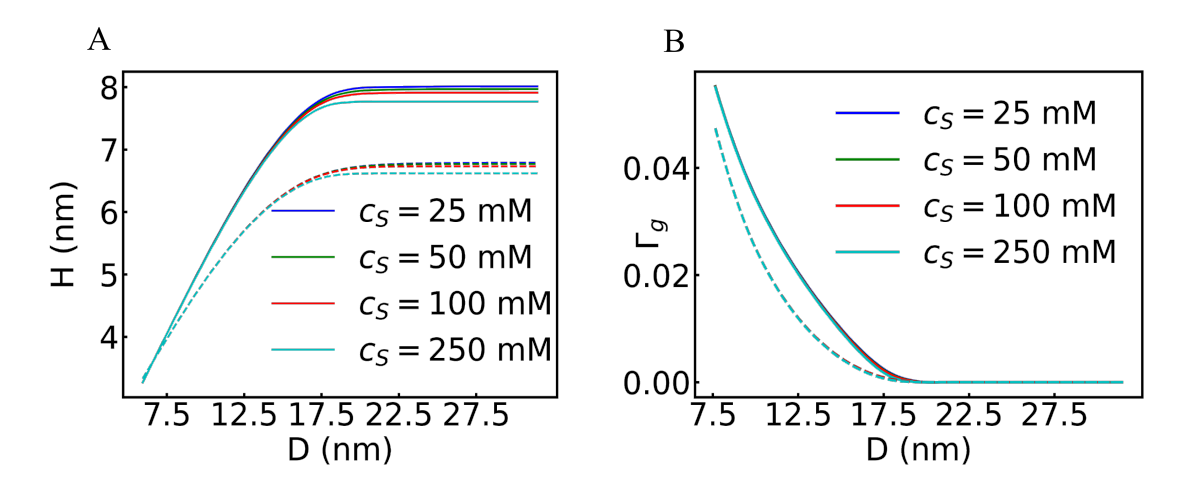


Figure 9: Variation of (A) the brush height and (B) interdigitation with the inter-plate separation for systems containing monovalent counterions. The solid lines are cDFT results and the dashed lines are from mean-field predictions.

ual chains (Fig.S1 in SI). A careful look at the corresponding detachment pressure versus distance curves reveals that this region coincides with the region of inter-brush attraction (Figure 6). This feature is however absent in the mean-field predictions.

As mentioned above, the extension of a charged brush is dictated by an interplay between the chain conformational entropy, intra-chain electrostatic repulsion between monomers, inter-chain electrostatic repulsion between monomers and excluded volume interactions. While electrostatic repulsion is described in the mean-field approach through an electrostatic potential, it only captures the long-range part through the net local charge density in the Poisson equation, neglecting individual short-range interactions dependent on size of charged species. It is therefore natural that the mean-field method underestimates the electrostatic repulsion between monomers in close spatial proximity. Additionally, the mean-field method neglects the excluded volume interactions, which result in decreased values of the brush height. It should be pointed out that the lack of explicit consideration of monomer-counterion correlation in the mean-field theory should predict a higher brush height since multivalent ions are known to collapse polyelectrolyte brushes. While cDFT predicts that the brush height is smaller for higher counterion valencies, the notable observation that, when correlations are considered, the brush height is elevated, suggests that the brush-brush

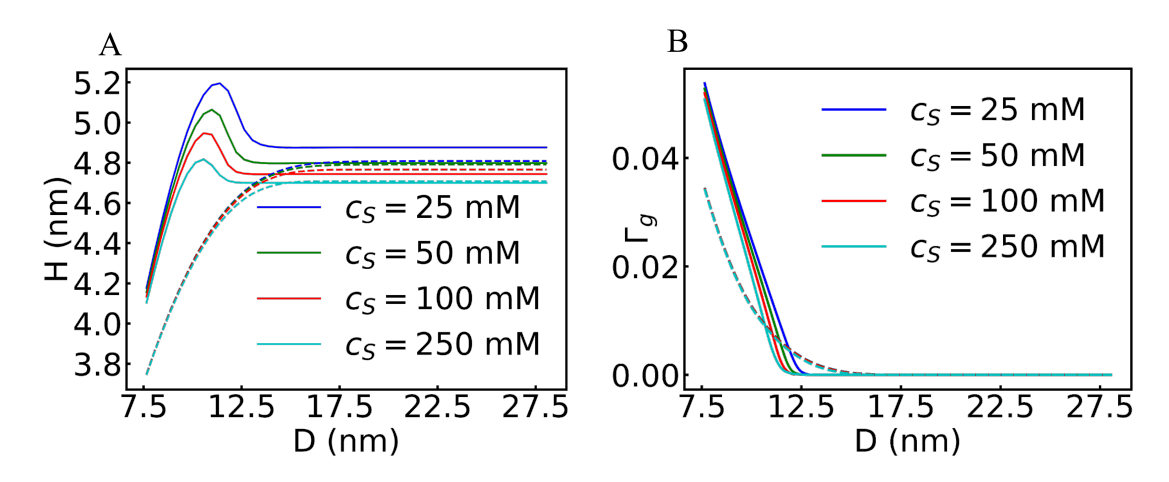


Figure 10: Variation of (A) the brush height and (B) interdigitation with the inter-plate separation for systems containing trivalent counterions. The solid lines are cDFT results and the dashed lines are from mean-field predictions.

interactions are overwhelmed by inter-brush attraction in addition to the excluded-volume repulsion. Another prominent driving force behind the observed behavior is the organization of counterions in the region between two brushes. The interaction of these counterions with monomers of opposing brushes pulls the chains of opposing brushes towards each other, as shown in monomer density profiles to be discussed later, causing an increase in the brush height and an attractive interaction. At very low separation distances, the excluded volume interactions between monomers become dominant, leading to an invariance of the brush height with the salt concentration.

The above observations on the brush heights are also reflected in the degree of interdigitation. The right panels in Figures 9 and 10 show the degree of interdigitation versus the inter-plate distance for both the monovalent and trivalent systems at all studied salt concentrations. It is seen that the distance at the onset of overlap between two brushes, signified by a non-zero degree of interdigitation, is lowered while going from the monovalent system to the trivalent system. This is due to the multivalent ion's enhanced ability to collapse brush through interlink formation between monomers, which makes them behave like neutral brushes. The monomer and counterion density profiles also corroborate this claim. The profiles are flatter for monovalent ions than for trivalent ions and there is enhanced

segregation of monomers at the midplane. It is also seen that correlation effects bring chains towards the center causing enhanced inter-brush overlap while in the absence of them, the monomer density profiles display two peaks, one near each wall. Additionally, it is also clear that for both monovalent and trivalent systems, counterion profiles closely follow those of the polymer segments, leading to the brush overlap. This is indicative of an osmotic brush where there is strong condensation of counterions onto each monomer. In the monovalent system, the monomer density and the counterion density are nearly constant throughout the brush. Previously, MD simulations on opposing polyelectrolyte brushes showed that monomer density profiles and counterion density profiles overlap for osmotic brushes. 32 We find in this work that, as the brushes were compressed against each other, the profiles became flatter. It was also observed that there is a slight lowering of density values at the center of the inter-plate region, accompanied by a small deviation between monomer and counterion density profiles. This feature is seen only to a small degree in our monomer density profile since the gap is small.

At small distances when the brushes physically overlap, the dominance of excluded volume interactions makes the detachment pressure insensitive to the salt concentration. This is the primary reason why the cross-over distance from repulsion to attraction varies negligibly with salt concentration. However, at larger distances where the brushes are far apart, the salt concentration becomes an important factor. This is clear from the brush height vs. distance plots in the panel A of Figure 10, which shows the brushes to be extending at low salt concentration. This plot also explains why the depth as well as the width of attraction valley reduce with increasing salt concentration and why any changes to the pressure-vs-distance curves in terms of the onset of attraction occur in their outer regions. The slight increase in the value of cross-over distance with increasing salt concentration can be explained on the basis of reduced interlink formation tendency of brushes under high salt concentrations.

A comparison of Figures 9 and 10 showed that, at similar conditions, the monovalent ion system exhibits a higher degree of interdigitation. If that is the case, why does the attraction between the opposing brushes take place in the trivalent systems? To resolve these two seemingly conflicting observations, we examine the electrostatic potential ($\beta\Psi$) profiles for these two valencies for D=9.4 nm and $c_S=25$ mM in Figure 11. It is seen that $\beta\Psi$ changes sign from negative to positive when the counterion valency is increased from 1 to 3. There is also a reduction in the absolute magnitude of electrostatic potential accompanying this sign change, which signals charge reversal within the brushes due to trivalent ion binding. The reduced magnitude is indicative of reduced electrostatic repulsive energy. It is therefore prudent to emphasize that in determining conditions for attraction and repulsion between two brush layers for anti-friction applications, the degree of interdigitation alone should not be viewed as the primary metric for determining the inter-brush repulsion or attraction, and one must consider the complete picture of interactions through the grand potential of the entire system.

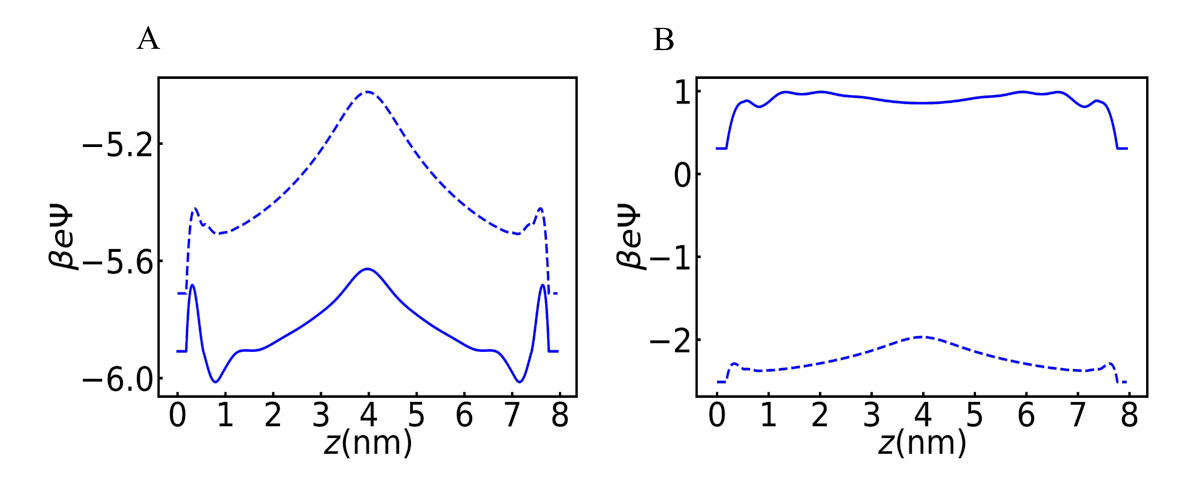


Figure 11: The local electrostatic potential for the brush systems with monovalent (A) and the trivalent (B) counterions considered in Figures 7 and 8.

Reentrant behavior of inter-brush attraction

In the previous sections, it was seen that though in the divalent and trivalent salt systems, there is attraction between opposing brushes, the magnitude of attraction diminishes with increasing salt concentration. In the past studies, ^{52,53} the ability of multivalent counterions

to produce attraction between same-charged spherical macroions was found to be highest at intermediate concentrations of counterions. However, numerical convergence in cDFT becomes hard to achieve at most separation distances under low salt concentrations due to high electrostatic repulsion, obscuring the observation of reentrant behavior. Therefore, we use monovalent salt at a sufficiently high concentration as the base counterion to mitigate the repulsion and add trivalent counterions starting from a small concentration as a method to realize reentrant behavior.

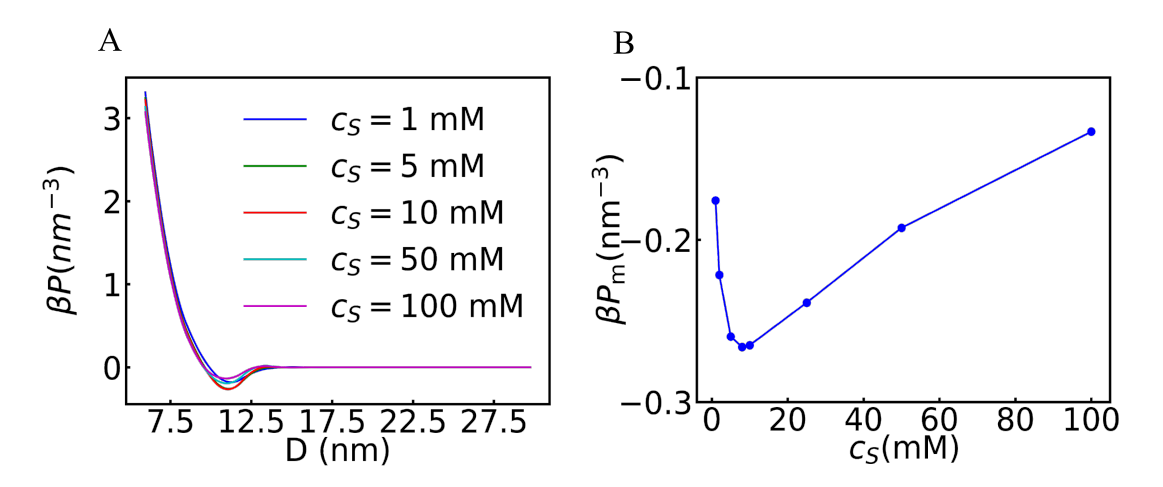


Figure 12: (A) The effect of trivalent salt concentration on the detachment pressure at a fixed monovalent salt concentration of 150 mM. (B) The variation of maximum attraction with the trivalent salt concentration.

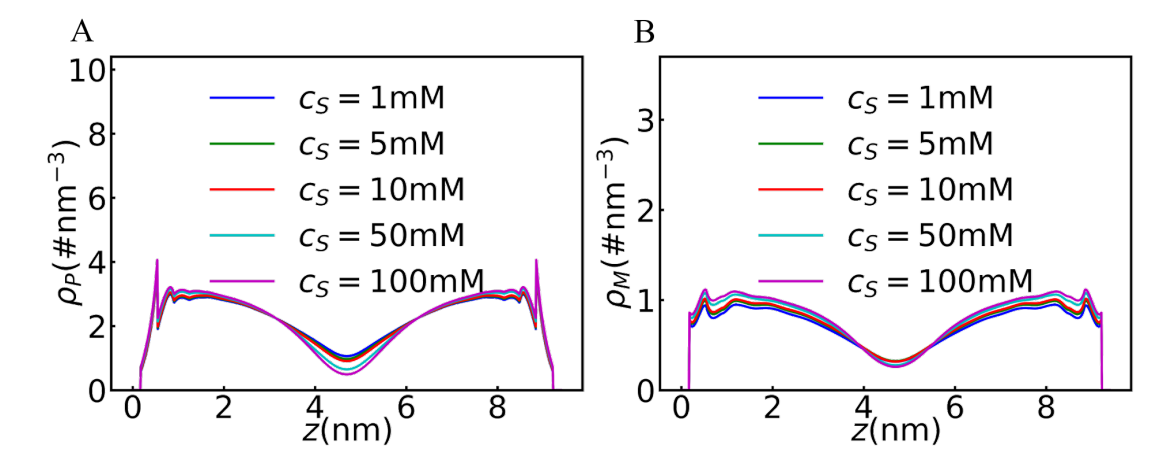


Figure 13: The effect of trivalent salt concentration on (A) the monomer density profiles (B) the trivalent counterion density profiles at a fixed monovalent salt concentration of 150 mM.

Figure 12 presents the variation of the detachment pressure with the concentration of trivalent ions at different inter-plate separations. Here the system also contains at a monovalent salt with a fixed concentration of 150 mM. The right panel in the same figure shows the strength of the maximum attraction versus the trivalent ion concentration. As was anticipated, the addition of trivalent ions initially deepens the trough in the pressure-vsdistance curves, indicating enhanced attraction. However, beyond 8 mM, it has an opposite effect. To understand the above trend by means of structural changes in the brush, we plot in Figure 13 the density profile of polymer segments and that of the trivalent counterions at different trivalent ion concentrations in the bulk solution. As the concentration of trivalent ions increases, the density profile of polymer segments becomes more localized towards the two grafting surfaces. A similar trend is observed for the counterion density profiles. This behavior is the same as what was observed for single component salt solutions and hence, it does not explain the non-monotonic dependence of the maximum attraction on the salt concentration. Earlier, the reentrant behavior upon the addition of multivalent ions was observed in the swelling of polymer gels. 11 Here, monomer-ion correlation effects dominate the thermodynamics at low salt concentrations, while the excluded volume effects become dominant at high salt concentrations. However, in our work, due to the absence of a non-monotonic trend in the density profiles, we refrain from attributing the origin of the reentrant behavior to a competition between excluded volume effects and electrostatic interaction. In this context, we believe a detailed study based on molecular dynamics simulation would prove useful since it allows for the direct quantification of intra-brush and inter-brush monomer-ion interlinks, which can be then examined as a function of salt concentration.

Effect of polyelectrolyte grafting density and chain length

Grafting density represents the denseness of a brush and dictates the relative effects of electrostatic and excluded volume interactions within a polyelectrolyte brush. In a previous cDFT study on single-brush systems under trivalent salt conditions, ⁵¹ the thickness of the brush

was found to initially decrease due to the increased number of interlinks between monomers and later increase with increasing grafting density due to excluded volume interactions. To investigate how this competition mediates interaction between two opposing brushes, we vary the grafting density for systems with monovalent and trivalent ions. Figure 14 shows the detachment pressure versus brush separation for these two valencies at $c_S = 50$ mM. It is seen that for both cases, increasing σ_g strengthens the repulsive part of the detachment pressure. This is expected due to higher number of charged monomers at higher grafting densities, leading to more repulsion due to electrostatic as well as excluded volume effects at small separations. Similarly, for monovalent counterions, the detachment pressure is purely repulsive, which is also obvious. However, the most prominent feature in the curves is that for trivalent ions, although increasing the grafting density shifts the minimum of the detachment pressure vs distance curve towards a higher value of D, negligible change occurs in the depth of the minimum, i.e., the maximum strength of attraction between two brushes. For trivalent counterions, the correlation effects are quite strong and hence attraction between opposing brushes can be realized with a small amount of monomers. As the grafting density increases, there is an increased repulsion between monomers while the number of monomercounterion crosslinks remains the same. This shifts the minimum in the detachment pressure versus distance curves to higher values. A useful way to prove this hypothesis would be to examine the density profiles of monomers and counterions at respective minimums, which are shown in Figure 15. It is seen that for the lowest three grafting densities considered in this work, the density profiles converge almost to a single value at the mid-plane and for $\sigma_g = 0.9 \text{ nm}^{-2}$, the densities of both monomers and counterions at the mid-plane are slightly lower than the corresponding value for the first three grafting densities. This invariance of both monomer and counterion densities in the midplane with respect to grafting density for the lowest three values of σ_g can be safely taken as the signature of constancy of the number of monomer-counterion contacts, which proves the hypothesis presented before. At $\sigma_g = 0.9 \text{ nm}^{-2}$, however, we believe the brushes retract into themselves due to high electrostatic repulsion between monomers from opposing brushes, and the reduced repulsion from this retracted arrangement of brushes explains why the attraction strength remains more or less the same with reduced interlinks.

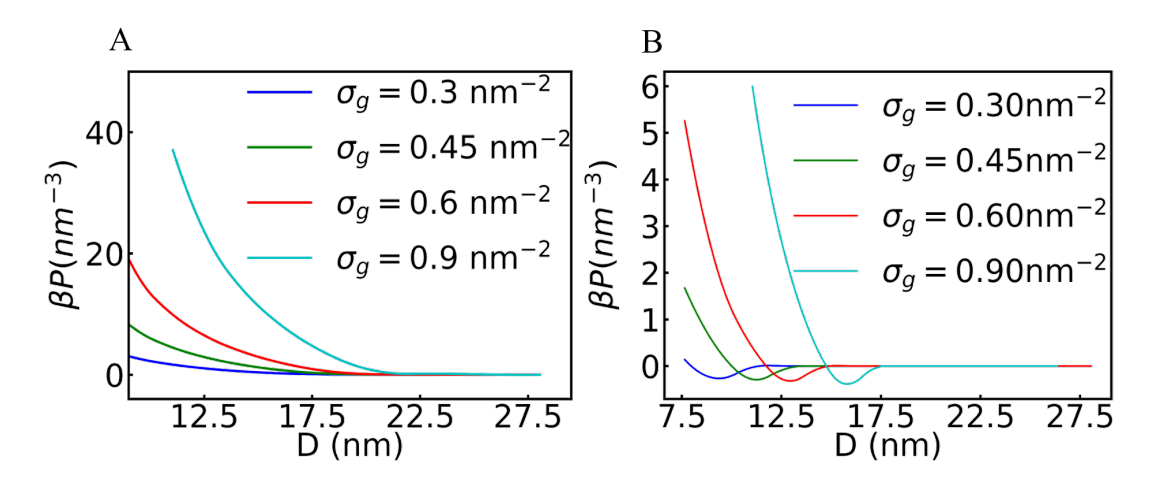


Figure 14: The effect of polyelectrolyte grafting density on the detachment pressure between opposing brushes in monovalent (A) and trivalent (B) electrolyte solutions. In both cases, the salt concentration is fixed at 50 mM.

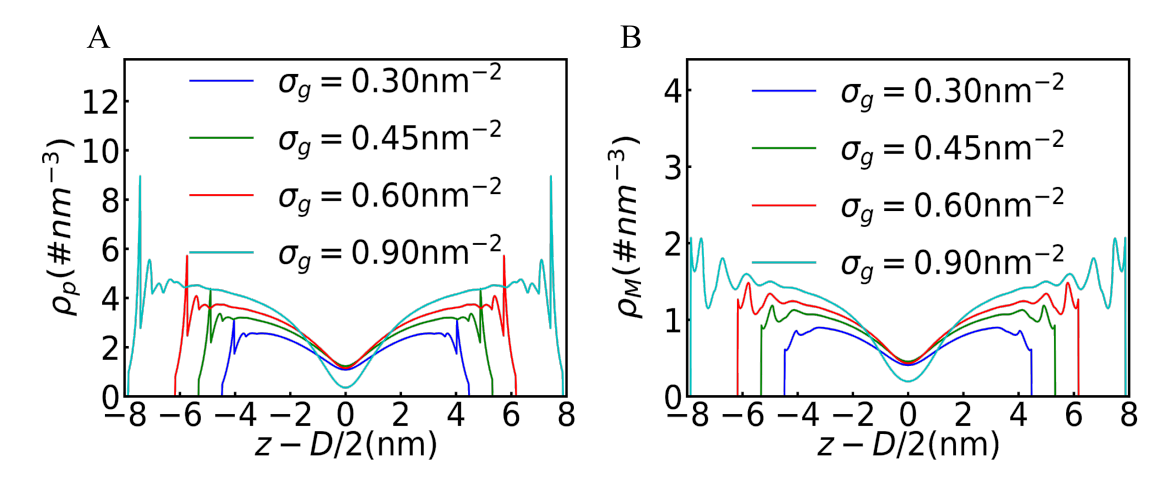


Figure 15: The effect of grafting density on the monomer density profiles (A) and the counterion density profiles (B) at distances corresponding to minima in Figure 14 (B). Here the counterions are trivalent.

The saturation of electrostatic correlation effect is also seen with the variation of the polymer length. Figure 17 shows the pressure vs distance plots for different polyelectrolyte brushes at $c_S = 50$ mM for the trivalent counterion system. As was the case with graft-

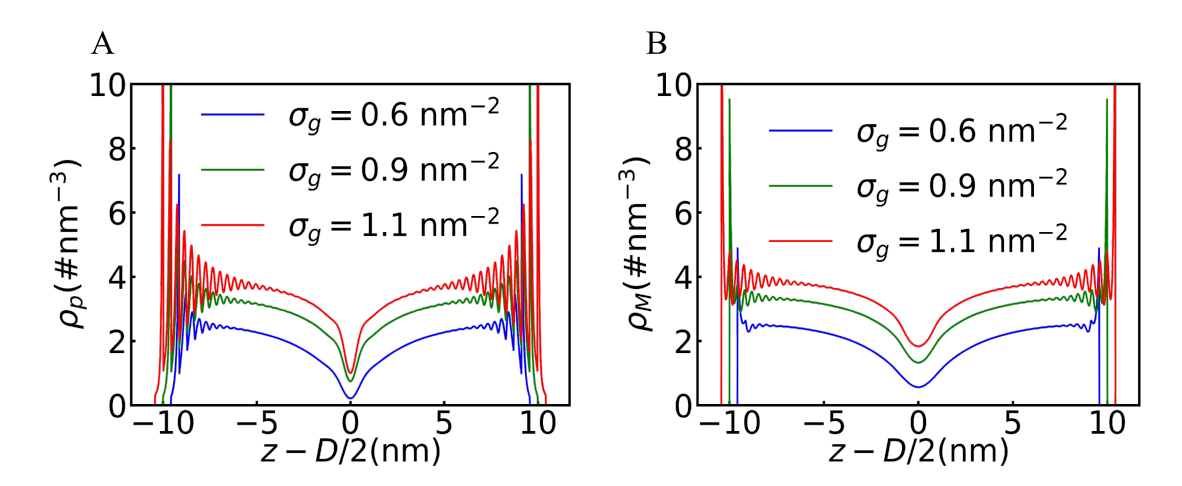


Figure 16: The effect of grafting density on the monomer density profiles (A) and the counterion density profiles (B) at distances corresponding to minima in Figure 14 (A). Here, the systems contain only monovalent counterions, and $\sigma_g = 0.3 \text{ nm}^{-2}$ is not considered since the pressure is positive at all distances.

ing density variation, increasing chain length only serves to shift the location of maximum attraction toward higher separation values while the depth of the attraction stays virtually unaffected. This can again be explained in terms of the saturation of electrostatic correlation as both increasing the grafting density and increasing the chain length have the same effect of increasing the amount of monomers. The increased monomer amount enhances electrostatic repulsion, hence the minimum in the detachment pressure vs distance plots moves towards higher separation distances. This is reflected in the monomer and counterion density profiles for three chain lengths (given in Figure 18) at distances corresponding to their respective minima. Here, a higher chain length enhances the concentrations of both species in the midplane, increasing both electrostatic repulsion and monomer-counterion contacts. These two effects balance each other and the maximum attraction strength does not vary significantly.

The invariance of maximum attractive strength between brushes with respect to grafting density and chain length was earlier noted by Rikkert and coworkers in polyacrylic acid brushes in a mixture of calcium and sodium counterion solution probed through a molecular theory. ²⁴ While that study was concerned with weak polyelectrolytes and the treatment of counterion-monomer correlation followed a chemical reaction formalism, the agreement be-

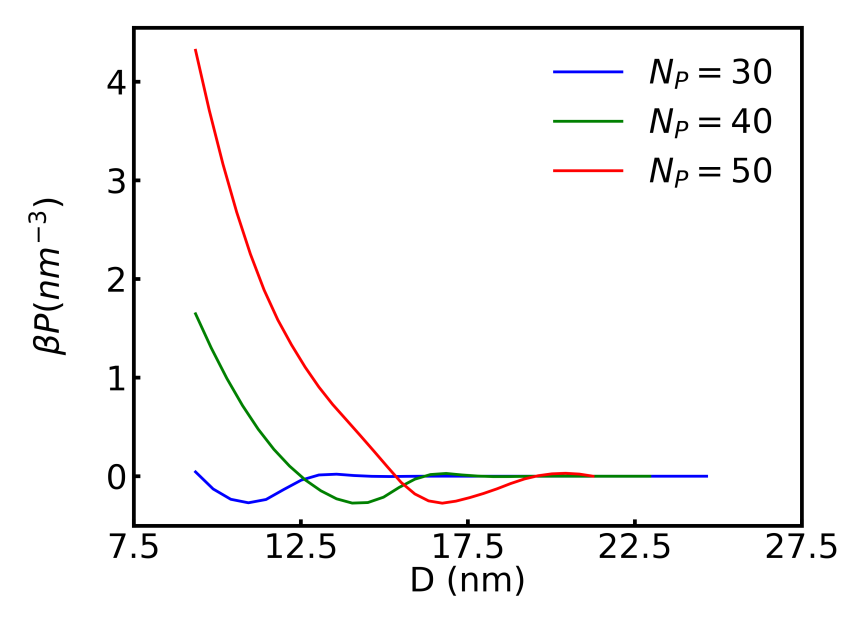


Figure 17: The effect of chain length on the detachment pressure between polyelectrolyte brushes in the presence of a trivalent salt at concentration of 50 mM.

tween our and their systems establishes the enhanced role of counterion-monomer correlation even at small concentrations in multivalent ion systems. It also reflects the simplicity yet effectiveness of cDFT in capturing bridging interactions with no special assumptions about the nature of monomer-counterion interactions.

Effect of counterion size

Finally, in this subsection, we investigate how counterion size can be used to tune the interaction between two polyelectrolyte brushes. Surface force experiments from the literature suggest that size variation of counterions can change the interaction force from repulsive to attractive.⁵⁴ Previous theoretical investigations also indicate that changing the counterion size changes the response of brush height to the grafting density in single brush systems.²⁹

To see how the effect of counterion size is manifested in the two-brush system, we plot in Figure 19 the detachment pressure vs separation for three different counterion diameters (σ_M), keeping the monomer and coion sizes equal to each other and constant at 0.425 nm.

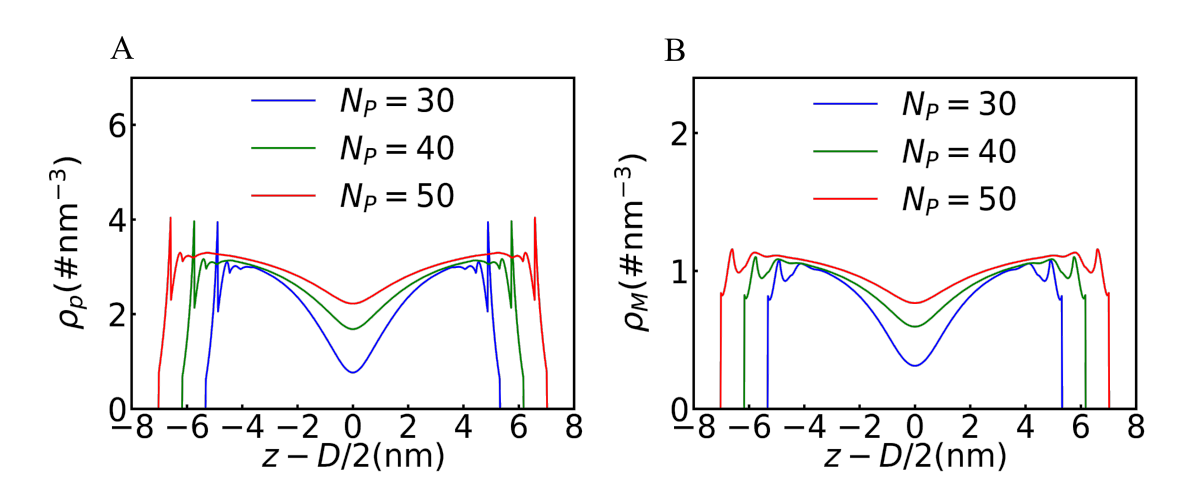


Figure 18: (A) Monomer density profiles and (B) counterion density profiles as a function of chain length. The separation distances correspond to those at the minimums of βP vs D curves in Figure 17.

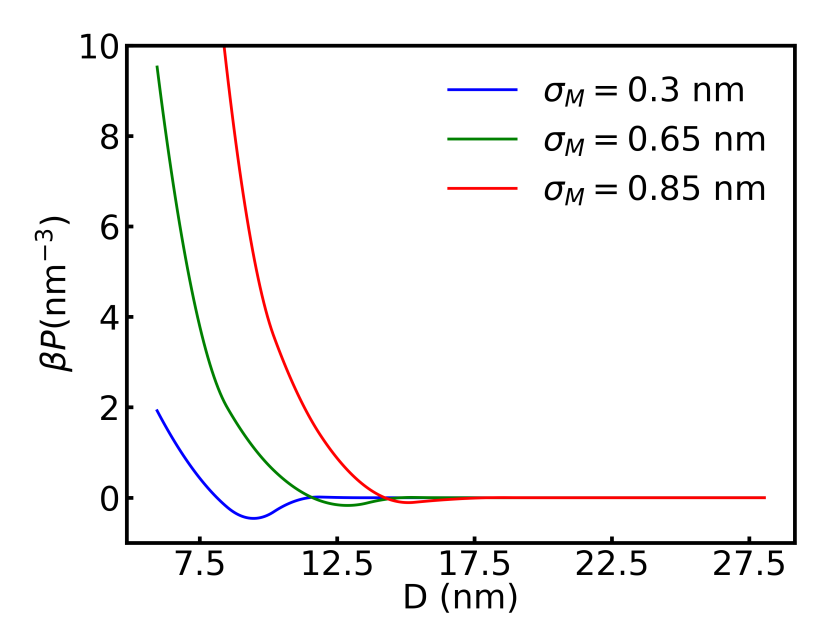


Figure 19: The effect of trivalent counterion size on the detachment pressure between opposing polyelectrolyte brushes. Here the trivalent salt concentration is fixed at 50 mM.

It is clear in these plots that increasing the counterion size enhances the repulsive part of the curves and reduces both the depth and width of the attractive valley. The increase in the counterion diameter also increases the separation distance corresponding to maximum attraction. The role of counterion size is primarily due to the Coulomb energy of monomerion interaction, which has an inverse dependence on the sum of radii of charged species involved. Hence, smaller counterions generate higher amounts of attraction and are more effective at bridging the oppositely charged monomers.⁵⁴ It might also be possible that large-sized counterions create a high amount of excluded volume repulsion within a brush, stretching the chains towards the center, which in turn leads to a high amount of electrostatic repulsion as well as excluded volume repulsion.

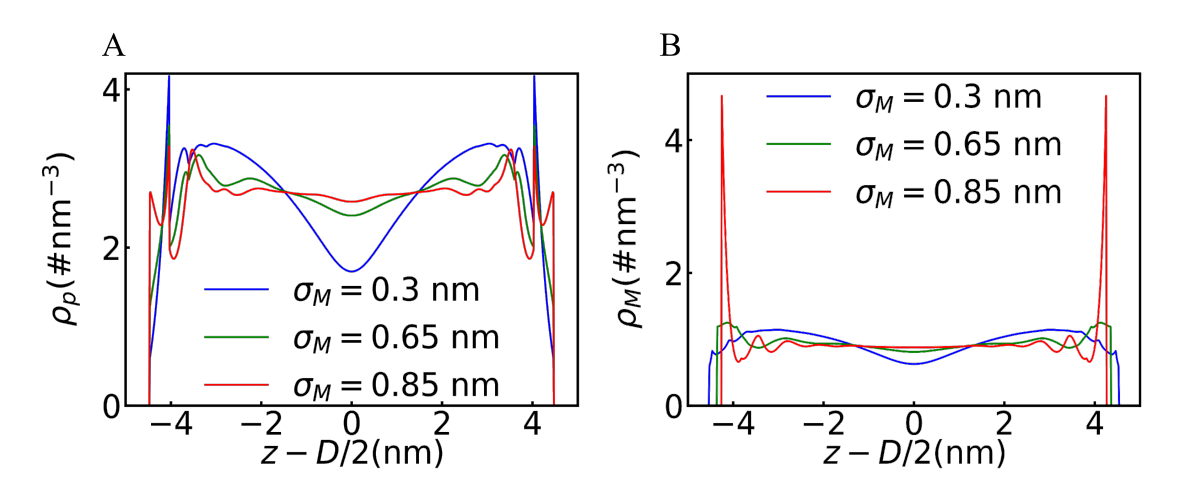


Figure 20: The effect of trivalent counterion size on the monomer density profiles (A) and the counterion density profiles (B) at D=9.4 nm. This distance corresponds to the minimum in the detachment pressure vs separation for $\sigma_M=0.3$ nm in Figure 19.

It has been shown previously that, in a neutral counterpart system, varying the asymmetry between grafted monomer size and the monomer size of free polymer chains shifts the boundary between attraction and repulsion. ⁴⁴ Specifically, larger grafted monomers resulted in greater repulsion due to enhanced excluded volume interactions. To delineate the roles of both interactions, we show in Figure 20 the monomer density for three counterion diameters at D = 9.4 nm. It is clear that for $\sigma_C = 0.85$ nm, the monomer profile is flat in the middle and for $\sigma_C = 0.30$ nm, there is bifurcation into two separate peaks towards the two walls, indicating low inter-brush overlap (Fig. S2).

Additionally, to probe the physics behind the highest amount of attraction for the smallest counterion, we present in Figure 21 the monomer and counterion density profiles at distances corresponding to the minima in respective βP versus D curves. It is seen that both the

monomer density and the counterion density at the mid-plane are highest for $\sigma_M = 0.30$ nm, hinting at highest amount of interlinks along the lines of the argument presented in the previous section. This means that there is enough counteracting force against electrostatic repulsion due to high monomer density, which is the reason that the location of the minimum occurs at a smaller separation than for other sizes.

The above observations are consistent with previous experimental reports. For example, in surface force apparatus experiments on sodium polystyrene sulphonate brushes under constant monovalent salt concentrations, Tirrel and coworkers⁵⁴ observed a high amount of adhesion on La^{3+} addition compared to $Ru(NH_3)_6^{3+}$ and Al^{3+} . La^{3+} has a small hydration radius (0.31 nm) while the complex ion $Ru(NH_3)_6^{3+}$ and Al^{3+} (0.48 nm) have higher radii, which correspond to more resistance towards interlink formation. ⁵⁴ Additionally, experiments on divalent counterions, Ca²⁺, Ba²⁺ and Mg²⁺, also revealed an inverse correlation between brush height, which in turn is inversely correlated with monomer-counterion bridging interactions, and counterion size. 27 This agreement between our theoretical results and experiments underscores the ability of cDFT to capture size-induced correlation effects, which are missing in traditional mean-field theories.

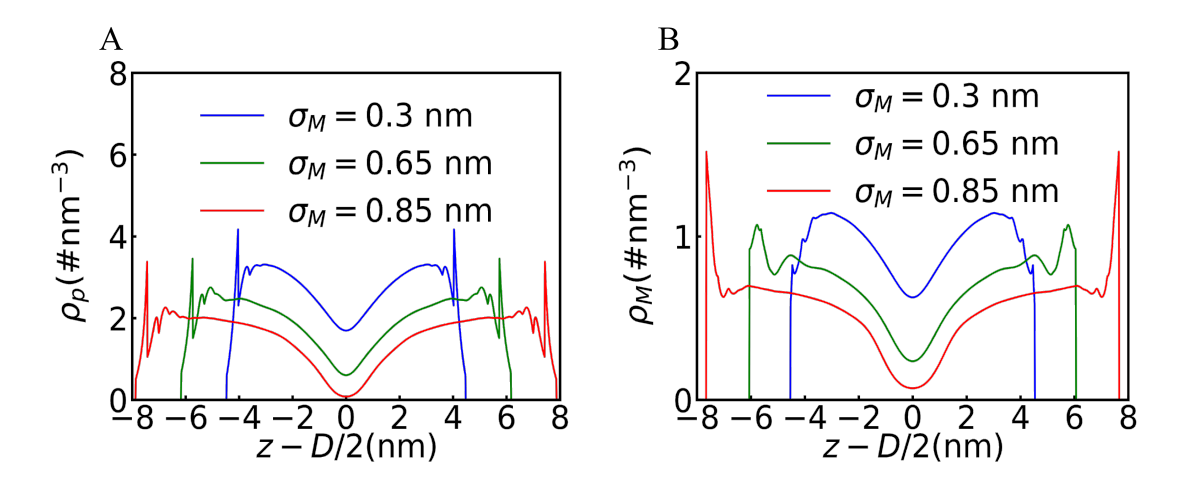


Figure 21: The effect of trivalent counterion size on the monomer density profiles (A) and the counterion density profiles (B) at distances corresponding to minima in Figure 19.

We note in a previous theoretical study for isolated brushes²⁹ that increasing the trivalent

counterion size was seen to reduce the height of the polyelectrolyte brush. However, the grafting density for the calculations was low and towards the higher ends of the spectrum, a crossover began to emerge. When the grafting density is low, the neighboring chains are far apart and cannot form interlinks unless the counterion is big enough to bridge them. It is for this reason that even though the strength of electrostatic attraction is low for large counterions, a collapse of the brush is observed with them and one sees an inverse relationship between the brush height and counterion size. However, when the grafting density becomes sufficiently high so that neighboring chains start to overlap considerably, excluded volume effects become significant and larger counterions cause the brush expansion. However, to study the size effect comprehensively with cDFT at a range of grafting densities, one dimensional theory might be inadequate due to the breakdown of lateral homogeneity assumption and hence, we do not pursue this study here.

Conclusions

In this work, we have used the classical density functional theory (cDFT) to study the interaction between two strongly charged polyelectrolyte brushes through the detachment pressure. The studied parameters were salt concentration, counterion valency, chain length, grafting density and counterion size. To highlight the importance of correlation effects, we have also presented comparisons with mean-field theory results. We observe that, regardless of the ion valencies, the mean-field theory predicts a stronger repulsion due to the neglect of ionic correlations, which are mostly attractive in nature. In contrast, cDFT is able to predict attraction between brushes for trivalent ions, which is not possible to capture in the mean-field framework. We also found that the detachment pressure displays a reentrant type behavior upon addition of multivalent salt, and that the attraction is maximum at an intermediate salt concentration. On varying chain length and grafting density for trivalent ions, we saw that the attraction strength remains the same while the location of the maximum

in attraction moves towards higher separation distances. On the other hand, for monovalent ions, we noticed that an increase in the strength of inter-brush attraction upon increasing the grafting density. Lastly, we discovered that increasing the size of counterions reduces the attractive part of the interaction between opposing polyelectrolyte brushes mediated by multi-valency counterions.

Where the effect of multivalent ions on adhesion between opposing polyelectrolyte brushes has been explored experimentally in the past, a systematic theoretical investigation of this intriguing behavior was missing. While there were a limited number of theoretical studies on such systems, either they were simulation based, which can be time-consuming or they involved assumptions about ion-pair interactions. Our work is therefore the first theoretical exploration of such systems involving little to no assumptions regarding the nature of interactions between monomers and counterions. Although a direct comparison of the numerical results have not been attempted, we find good qualitative agreement between the theoretical results and experimental observations with regard to the general trends such as the effect of salt concentration and valency on the brush thickness and inter-brush potential.

A few possible extensions of our work are possible. First, one can try to study the interaction between oppositely charged polyelectrolytes. While intuitively the interaction between them is expected to be attractive, strong correlation effects have been seen to induce repulsion between oppositely charged bare surfaces ^{55,56} and hence, can be anticipated to cause significant changes quantitatively with respect to parameters such as salt amount, etc. Studying interaction between oppositely charged brushes would have direct relevance with the design of adhesives and the assembly of oppositely charged colloids in water. ⁵⁷ Second, an exploration of the polymer sequence effects, e.g., by various combinations of either charged and neutral monomers or positively charged and negatively charged monomers in the brushes, can be carried out to obtain conditions for maximum adhesion or lubrication. A third direction would be to conduct the cDFT study in three dimensions to investigate the appropriateness of the assumption of lateral homogeneity. In the current study, we did

not consider dilute brushes since in such systems, the assumption of lateral homogeneity breaks down. Additionally, lateral heterogeneity also becomes important for brush coated nanoparticles since the chains on a surface can splay apart as the brushes approach each other. Here, a three-dimensional study would be a major advancement in our quest to obtain a comprehensive understanding of opposing brush systems. Finally, a useful way to answer a few unresolved questions in the current work such as the physical phenomenon behind the observed reentrant behavior with respect to salt concentration would be to perform MD simulation and quantify the variation of inter-brush monomer-counterion interlinks with the salt concentration.

Acknowledgement

This research is made possible through financial support from the NSF-DFG Lead Agency Activity in Chemistry and Transport in Confined Spaces under Grant No. NSF 2234013. Furthermore, AG thanks additional financial assistance provided by the NSF Graduate Research Fellowship under Grant No. DGE-1326120.

Supporting Information:

Equations for excess free energy in density functional theory and additional figures for the segment density profiles of polymer brushes and the effect of trivalent counterion size on the interdigitation between opposing brushes.

References

(1) Levin, Y. Electrostatic correlations: from plasma to biology. Rep. Prog. Phys. 2002, 65, 1577.

- (2) Naji, A.; Kanduč, M.; Forsman, J.; Podgornik, R. Perspective: Coulomb fluids—Weak coupling, strong coupling, in between and beyond. *J. Chem. Phys.* **2013**, *139*, 150901.
- (3) Quesada-Pérez, M.; González-Tovar, E.; Martín-Molina, A.; Lozada-Cassou, M.; Hidalgo-Álvarez, R. Ion size correlations and charge reversal in real colloids. *Colloids Surf. A Physicochem. Eng. Asp.* **2005**, *267*, 24–30.
- (4) Russell, W. S.; Lin, C.-Y.; Siwy, Z. S. Gating with Charge Inversion to Control Ionic Transport in Nanopores. ACS Appl. Nano Mater. 2022, 5, 17682–17692.
- (5) Li, Y.; Girard, M.; Shen, M.; Millan, J. A.; Olvera de la Cruz, M. Strong attractions and repulsions mediated by monovalent salts. *Proc. Natl. Acad. Sci. U.S.A.* 2017, 114, 11838–11843.
- (6) Lozada-Cassou, M.; Henderson, D. The application of the hypernetted chain approximation to the electrical double layer. Comparison with Monte Carlo results for 2: 1 and 1: 2 salts. J. Phys. Chem. 1983, 87, 2821–2824.
- (7) Ravindran, S.; Wu, J. Overcharging of nanoparticles in electrolyte solutions. *Langmuir* **2004**, *20*, 7333–7338.
- (8) Balzer, C.; Jiang, J.; Marson, R. L.; Ginzburg, V. V.; Wang, Z.-G. Nonelectrostatic Adsorption of Polyelectrolytes and Mediated Interactions between Solid Surfaces. *Lang-muir* 2021, 37, 5483–5493.
- (9) Luque-Caballero, G.; Martín-Molina, A.; Quesada-Pérez, M. Polyelectrolyte adsorption onto like-charged surfaces mediated by trivalent counterions: A Monte Carlo simulation study. J. Chem. Phys. 2014, 140, 174701.
- (10) Wang, L.; Liang, H.; Wu, J. Electrostatic origins of polyelectrolyte adsorption: Theory and Monte Carlo simulations. *J. Chem. Phys.* **2010**, *133*, 044906.

- (11) Jha, P. K.; Zwanikken, J. W.; De La Cruz, M. O. Understanding swollen–collapsed and re-entrant transitions in polyelectrolyte nanogels by a modified Donnan theory. *Soft Matter* **2012**, *8*, 9519–9522.
- (12) Besteman, K.; Van Eijk, K.; Lemay, S. Charge inversion accompanies DNA condensation by multivalent ions. *Nat. Phys.* **2007**, *3*, 641–644.
- (13) Samanta, D.; Iscen, A.; Laramy, C. R.; Ebrahimi, S. B.; Bujold, K. E.; Schatz, G. C.; Mirkin, C. A. Multivalent cation-induced actuation of DNA-mediated colloidal super-lattices. J. Am. Chem. Soc. 2019, 141, 19973–19977.
- (14) Mei, Y.; Lauterbach, K.; Hoffmann, M.; Borisov, O. V.; Ballauff, M.; Jusufi, A. Collapse of spherical polyelectrolyte brushes in the presence of multivalent counterions. *Phys. Rev. Lett.* **2006**, *97*, 158301.
- (15) Yu, J.; Jackson, N. E.; Xu, X.; Brettmann, B. K.; Ruths, M.; De Pablo, J. J.; Tirrell, M. Multivalent ions induce lateral structural inhomogeneities in polyelectrolyte brushes. *Sci. Adv.* **2017**, *3*, eaao1497.
- (16) Lin, C.; Qiang, X.; Dong, H.-L.; Huo, J.; Tan, Z.-J. Multivalent Ion-Mediated Attraction between Like-Charged Colloidal Particles: Nonmonotonic Dependence on the Particle Charge. ACS Omega 2021, 6, 9876–9886.
- (17) Salerno, K. M.; Frischknecht, A. L.; Stevens, M. J. Charged nanoparticle attraction in multivalent salt solution: A classical-fluids density functional theory and molecular dynamics study. J. Phys. Chem. B 2016, 120, 5927–5937.
- (18) Kumar, S.; Yadav, I.; Abbas, S.; Aswal, V. K.; Kohlbrecher, J. Interactions in reentrant phase behavior of a charged nanoparticle solution by multivalent ions. *Phys. Rev. E* **2017**, *96*, 060602.

- (19) Wu, J.; Bratko, D.; Prausnitz, J. M. Interaction between like-charged colloidal spheres in electrolyte solutions. *Proc. Natl. Acad. Sci. U.S.A.* **1998**, *95*, 15169–15172.
- (20) Diehl, A.; Tamashiro, M.; Barbosa, M. C.; Levin, Y. Density-functional theory for attraction between like-charged plates. *Physica A* **1999**, *274*, 433–445.
- (21) Yu, J.; Jackson, N.; Xu, X.; Morgenstern, Y.; Kaufman, Y.; Ruths, M.; De Pablo, J.; Tirrell, M. Multivalent counterions diminish the lubricity of polyelectrolyte brushes. Science 2018, 360, 1434–1438.
- (22) Raviv, U.; Giasson, S.; Kampf, N.; Gohy, J.-F.; Jérôme, R.; Klein, J. Lubrication by charged polymers. *Nature* **2003**, *425*, 163–165.
- (23) Pincus, P. Colloid stabilization with grafted polyelectrolytes. *Macromolecules* 1991, 24, 2912–2919.
- (24) Nap, R. J.; Szleifer, I. Effect of calcium ions on the interactions between surfaces end-grafted with weak polyelectrolytes. *J. Chem. Phys.* **2018**, *149*, 163309.
- (25) Zhulina, E.; Borisov, O. Structure and interaction of weakly charged polyelectrolyte brushes: Self-consistent field theory. *J. Chem. Phys.* **1997**, *107*, 5952–5967.
- (26) Cao, Q.; Zuo, C.; He, H.; Li, L. A Molecular Dynamics Study of Two Apposing Polyelectrolyte Brushes with Mono-and Multivalent Counterions. *Macromol. Theor. Simulat.* 2009, 18, 441–452.
- (27) Yu, J.; Mao, J.; Yuan, G.; Satija, S.; Jiang, Z.; Chen, W.; Tirrell, M. Structure of polyelectrolyte brushes in the presence of multivalent counterions. *Macromolecules* **2016**, 49, 5609–5617.
- (28) Matsen, M. Effect of salt on the compression of polyelectrolyte brushes in a theta solvent. Eur. Phys. J. E 2012, 35, 13.

- (29) Jiang, T.; Wu, J. Self-organization of multivalent counterions in polyelectrolyte brushes. *J. Chem. Phys.* **2008**, *129*, 084903.
- (30) Kumar, N. A.; Seidel, C. Interaction between two polyelectrolyte brushes. *Phys. Rev.* E 2007, 76, 020801.
- (31) Wynveen, A.; Likos, C. N. Interactions between planar stiff polyelectrolyte brushes. *Phys. Rev. E* **2009**, *80*, 010801.
- (32) Desai, P. R.; Sinha, S.; Das, S. Polyelectrolyte brush bilayers in weak interpenetration regime: Scaling theory and molecular dynamics simulations. *Phys. Rev. E* **2018**, *97*, 032503.
- (33) Wynveen, A.; Likos, C. N. Interactions between planar polyelectrolyte brushes: effects of stiffness and salt. *Soft Matter* **2010**, *6*, 163–171.
- (34) Ibergay, C.; Malfreyt, P.; Tildesley, D. J. Interaction between two polyelectrolyte brushes: a mesoscale modelling of the compression. *Soft Matter* **2011**, *7*, 4900–4907.
- (35) Matsen, M. W. Compression of polyelectrolyte brushes in a salt-free theta solvent. *Eur. Phys. J. E* **2011**, *34*, 1–12.
- (36) Zhulina, E. B.; Rubinstein, M. Lubrication by polyelectrolyte brushes. *Macromolecules* 2014, 47, 5825–5838.
- (37) Wang, M.; Tong, C. A numerical study of two opposing polyelectrolyte brushes by the self-consistent field theory. *RSC Adv.* **2014**, *4*, 20769–20780.
- (38) Li, Z.; Wu, J. Density functional theory for polyelectrolytes near oppositely charged surfaces. *Phys. Rev. Lett.* **2006**, *96*, 048302.
- (39) Jönsson, B.; Broukhno, A.; Forsman, J.; Åkesson, T. Depletion and Structural Forces in Confined Polyelectrolyte Solutions. *Langmuir* **2003**, *19*, 9914–9922.

- (40) Wu, J.; Jiang, T.; Jiang, D.-e.; Jin, Z.; Henderson, D. A classical density functional theory for interfacial layering of ionic liquids. *Soft Matter* **2011**, *7*, 11222–11231.
- (41) Xu, X.; Cao, D.; Wu, J. Density functional theory for predicting polymeric forces against surface fouling. *Soft Matter* **2010**, *6*, 4631–4646.
- (42) Jiang, T.; Li, Z.; Wu, J. Structure and Swelling of Grafted Polyelectrolytes: Predictions from a Nonlocal Density Functional Theory. *Macromolecules* **2007**, *40*, 334–343.
- (43) Li, Z.; Wu, J. Density functional theory for planar electric double layers: Closing the gap between simple and polyelectrolytes. J. Phys. Chem. B 2006, 110, 7473–7484.
- (44) Jain, S.; Ginzburg, V. V.; Jog, P.; Weinhold, J.; Srivastava, R.; Chapman, W. G. Modeling polymer-induced interactions between two grafted surfaces: Comparison between interfacial statistical associating fluid theory and self-consistent field theory. J. Chem. Phys. 2009, 131, 044908.
- (45) Balastre, M.; Li, F.; Schorr, P.; Yang, J.; Mays, J. W.; Tirrell, M. V. A study of polyelectrolyte brushes formed from adsorption of amphiphilic diblock copolymers using the surface forces apparatus. *Macromolecules* **2002**, *35*, 9480–9486.
- (46) Abraham, T.; Giasson, S.; Gohy, J.-F.; Jérôme, R. Direct measurements of interactions between hydrophobically anchored strongly charged polyelectrolyte brushes. *Langmuir* 2000, 16, 4286–4292.
- (47) Block, S.; Helm, C. A. Single polyelectrolyte layers adsorbed at high salt conditions: polyelectrolyte brush domains coexisting with flatly adsorbed chains. *Macromolecules* **2009**, *42*, 6733–6740.
- (48) Block, S.; Helm, C. A. Conformation of poly (styrene sulfonate) layers physisorbed from high salt solution studied by force measurements on two different length scales. J. Phys. Chem. B 2008, 112, 9318–9327.

- (49) Block, S.; Helm, C. A. Measurement of long-ranged steric forces between polyelectrolyte layers physisorbed from 1 M NaCl. *Phys. Rev. E* **2007**, *76*, 030801.
- (50) Elmahdy, M. M.; Synytska, A.; Drechsler, A.; Gutsche, C.; Uhlmann, P.; Stamm, M.; Kremer, F. Forces of interaction between poly (2-vinylpyridine) brushes as measured by optical tweezers. *Macromolecules* **2009**, *42*, 9096–9102.
- (51) Jiang, T.; Wu, J. Ionic effects in collapse of polyelectrolyte brushes. *J. Phys. Chem. B* **2008**, *112*, 7713–7720.
- (52) Fujihara, S.; Akiyama, R. Attractive interaction between macroanions mediated by multivalent cations in biological fluids. *J. Mol. Liq.* **2014**, *200*, 89–94.
- (53) Wu, J.; Prausnitz, J. M. Generalizations for the Potential of Mean Force between Two Isolated Colloidal Particles from Monte Carlo Simulations. J. Colloid Interface Sci. 2002, 252, 326–330.
- (54) Farina, R.; Laugel, N.; Yu, J.; Tirrell, M. Reversible adhesion with polyelectrolyte brushes tailored via the uptake and release of trivalent lanthanum ions. J. Phys. Chem. C 2015, 119, 14805–14814.
- (55) Wu, J. Z.; Bratko, D.; Blanch, H. W.; Prausnitz, J. M. Interaction between oppositely charged micelles or globular proteins. *Phys. Rev. E* **2000**, *62*, 5273–5280.
- (56) Trulsson, M.; Jönsson, B.; Åkesson, T.; Forsman, J.; Labbez, C. Repulsion between Oppositely Charged Surfaces in Multivalent Electrolytes. *Phys. Rev. Lett.* 2006, 97, 068302.
- (57) Spruijt, E.; Bakker, H. E.; Kodger, T. E.; Sprakel, J.; Stuart, M. A. C.; van der Gucht, J. Reversible assembly of oppositely charged hairy colloids in water. Soft Matter 2011, 7, 8281–8290.

TOC Graphic

